1973

Optimal synthesis of active distributed RC low-pass filters

Robert Iman Egbert

Department:

OPTIMAL SYNTHESIS OF ACTIVE DISTRIBUTED RC LOW-PASS FILTERS

by

ROBERT IMAN EGBERT, 1950-

A THESIS

Presented to the Faculty of the Graduate School of the

UNIVERSITY OF MISSOURI - ROLLA

In Partial Fulfillment of the Requirements for the Degree

MASTER OF SCIENCE IN ELECTRICAL ENGINEERING

1973

Approved by

J. J. Bourgin (Advisor) E C Bertnolli

Charles Hatfield

ABSTRACT

Although synthesis procedures for active distributed RC networks are well developed, the approximation problem is largely unsolved. Previously proposed solutions have several disadvantages. A better solution to the approximation problem is obtained by developing an error expression involving the difference between the ideal specification and the exact realization, then minimizing this error by numerical techniques. The method is illustrated by designing a set of active distributed RC low-pass filters.

ACKNOWLEDGMENTS

The author wishes to thank his major advisor, Dr. Jack J. Bourquin, for his help throughout the author's graduate studies and, in particular, during the research leading to this thesis. In addition, the author is grateful to the many faculty members from various departments, who provided valuable suggestions during his research, and to Mrs. Eunice French for the typing of the manuscript. Finally, the author wishes to express a special thanks to his parents, who encouraged him throughout his graduate studies.

TABLE OF CONTENTS

TABLE OF CONTENTS (continued) PAGE

LIST OF ILLUSTRATIONS

LIST OF TABLES

LIST OF SYMBOLS

C	Total capacitance
c	Per-unit capacitance
d	Total length
j	$\sqrt{-1}$
P	Complex frequency variable in the cosh $\sqrt{RCs}$ plane
R	Total resistance
r	Per-unit resistance
s	Complex frequency variable in the s plane
T	Transfer function
w	Complex frequency variable in the exp $\sqrt{RCs}$
Y	Admittance
z	Impedance
λ	Complex frequency variable in the tanh $\sqrt{RCs}$ plane
ω	Angular frequency variable in the s plane

I. INTRODUCTION

There are many advantages to be gained by using distributed RC networks in integrated circuits. For example, on an integrated circuit chip a distributed RC network occupies approximately the same amount of space as a single lumped capacitor [1]. Thus, if a distributed RC network can be made to function in approximately the same way as a lumped resistor and capacitor, or even a group of resistors and capacitors, a saving of space as well as a reduction in the total number of elements in the circuit can be achieved [2]. Also, as is shown below, distributed RC circuits perform better than lumped circuits in some applications.

Unfortunately these advantages are somewhat offset by the mathematical complications that occur when distributed RC networks are used in circuit synthesis. As shown later, simple synthesis methods for distributed RC networks exist; thus, the majority of these complications occur in the approximation of a given ideal specification by some realizable network transfer function. For example, in the frequency domain the ideal specification may be in the form of a gain or impedance function. This function must be approximated by another function of ω that can be transformed into a realizable driving-point immittance or transfer function by the relationship $\omega = s/j$. For lumped circuits this problem

has largely been solved. However, realizable transfer functions or driving-point immittances for distributed RC circuits contain hyperbolic, exponential, or algebraic functions of $\sqrt{s}$ [3]. Therefore, in order to obtain a realizable transfer function the ideal specification should be approximated by hyperbolic or exponential functions of $\sqrt{j\omega}$. This is a non-trivial task.

One approach to the solution of this problem has been to find a realizable distributed RC transfer function that has approximately the same frequency response as that of a lumped network [1,4,5]. This is done either by matching the dominant poles of the distributed RC network to the poles of the lumped transfer function or by some means finding the distributed RC network transfer function that has the smallest deviation in frequency response from that of a given lumped network transfer function. The ideal specification is then approximated by a lumped transfer function, which can be obtained from design tables or by other means; then the lumped transfer function is approximated by the distributed RC transfer function.

Although this method produces good results, it has two main disadvantages. First of all, the end result is an approximation of an approximation. Also, this method limits the response of the distributed RC network to that of a lumped network. There is the possibility that in a different circuit the distributed RC network would approximate the desired specification much better than the approximation obtained by the lumped circuit.

The second approach to the approximation problem involves investigating the frequency responses of a number of different realizable distributed RC transfer functions [6,7,8]. Usually the transfer functions are of the same general form, and only one parameter is varied. The frequency responses are then plotted as a one-parameter family of curves. The design procedure is to choose the particular curve that best approximates the desired specification.

The major problem with this method is the limited number of curves available. Interpolation must be made between the available curves to get an estimate of the best approximation of the ideal specification.

The third approach to the problem is the one proposed in this paper. It is similar to the second approach mentioned above in that the transfer function that best approximates a desired specification is obtained. However, in this method a mathematical expression for the difference between the desired and the actual response is formulated. Then standard numerical optimization techniques are applied to minimize this difference and thus find the transfer function which has a frequency response that best approximates the desired specification in some sense.

The advantages of this approach are that it assures that the "best" approximation is obtained, it eliminates the need for a large number of plots, and it allows a set of filter design tables to be constructed for standard

filters such as low-pass, high-pass, and band-pass, similar to those for lumped networks.

This paper develops a general expression for the function to be minimized and illustrates the method by designing a set of active distributed RC low-pass filters with a corresponding design table to simplify the synthesis. This table is then used to construct an actual circuit, and the performance is compared with the theoretical results.

II. REVIEW OF THE LITERATURE

A. DISTRIBUTED RC NETWORKS

1. Electrical Characteristics

A distributed network can be defined as an element for which the current-voltage relations must be described by partial differential equations [9]. A distributed RC network can be represented by the incremental model shown in Figure 1 and is described by the following equations [10]:

$$\frac{\partial v}{\partial x} = -r(x)\,i \tag{2.1a}$$

$$\frac{\partial i}{\partial x} = -c(x)\,\frac{\partial v}{\partial t} \tag{2.1b}$$

where $r(x)$ and $c(x)$ are the resistance and capacitance at point x along the line; x is measured from a zero reference at the input terminal of the network.

If the network is a uniformly distributed RC network ($\overline{\text{URC}}$), that is, if the resistance and capacitance are independent of x, then equations (2.1a) and (2.1b) become

$$\frac{\partial v}{\partial x} = -r_o\,i \tag{2.2a}$$

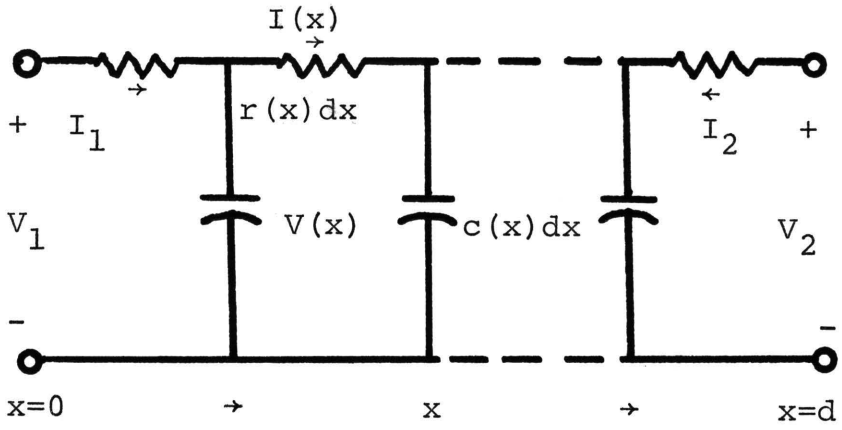

Figure 1. Incremental Model of an RC Line

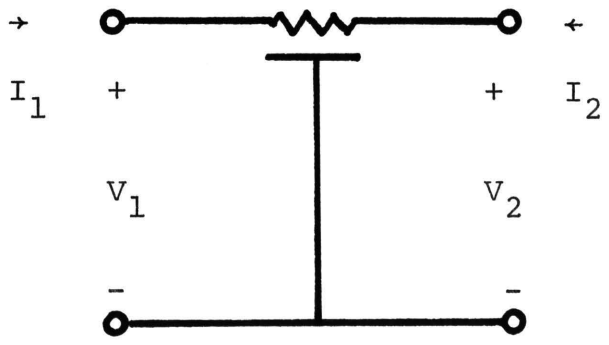

Figure 2. Circuit Symbol for a $\overline{\text{URC}}$ Two-Port Network

$$\frac{\partial i}{\partial x} = -c_o \frac{\partial v}{\partial t} \tag{2.2b}$$

where r_o and c_o are the constant per unit length values of resistance and capacitance, respectively. If r(x) and c(x) are not constants the network is called a tapered distributed RC network. If the $\overline{URC}$ is considered a two-port network as symbolized in Figure 2, and the terminal voltages and currents are taken as the boundary conditions, the resulting solutions of equations 2.2 can be expressed as the ABCD parameters of a URC of length d which are [11]

$$\begin{bmatrix} V_1 \\ I_1 \end{bmatrix} = \begin{bmatrix} \cosh\sqrt{r_o c_o d^2 s} & \sqrt{\frac{r_o}{sc_o}}\sinh\sqrt{r_o c_o d^2 s} \\ \sqrt{\frac{sc_o}{r_o}}\sinh\sqrt{r_o c_o d^2 s} & \cosh\sqrt{r_o c_o d^2 s} \end{bmatrix} \begin{bmatrix} V_2 \\ -I_2 \end{bmatrix} \tag{2.3a}$$

where

$$\begin{bmatrix} V_1 \\ I_1 \end{bmatrix} = \begin{bmatrix} A & B \\ C & D \end{bmatrix} \begin{bmatrix} V_2 \\ -I_2 \end{bmatrix} . \tag{2.3b}$$

These may readily be converted into the z and y matrices which are, respectively, [9,10]:

$$\begin{bmatrix} V_1 \\ V_2 \end{bmatrix} = \sqrt{\frac{R}{sC}} \begin{bmatrix} \coth \sqrt{RCs} & \operatorname{csch} \sqrt{RCs} \\ \operatorname{csch} \sqrt{RCs} & \coth \sqrt{RCs} \end{bmatrix} \begin{bmatrix} I_1 \\ I_2 \end{bmatrix} \tag{2.4}$$

$$\begin{bmatrix} I_1 \\ I_2 \end{bmatrix} = \sqrt{\frac{sC}{R}} \begin{bmatrix} \coth \sqrt{RCs} & -\operatorname{csch} \sqrt{RCs} \\ -\operatorname{csch} \sqrt{RCs} & \coth \sqrt{RCs} \end{bmatrix} \begin{bmatrix} V_1 \\ V_2 \end{bmatrix} \tag{2.5}$$

where $R=r_o d$ and $C=c_o d$.

2. Physical Characteristics

Physically, $\overline{URC}$ networks are of two types. A thin film $\overline{URC}$ is constructed as shown in Figure 3 [10]. A conducting film is deposited on a substrate followed by a dielectric, and a resistive layer is placed on top. The structure shown in Figure 4 is a pn-junction distributed network [2]. It consists of a revese-biased junction with

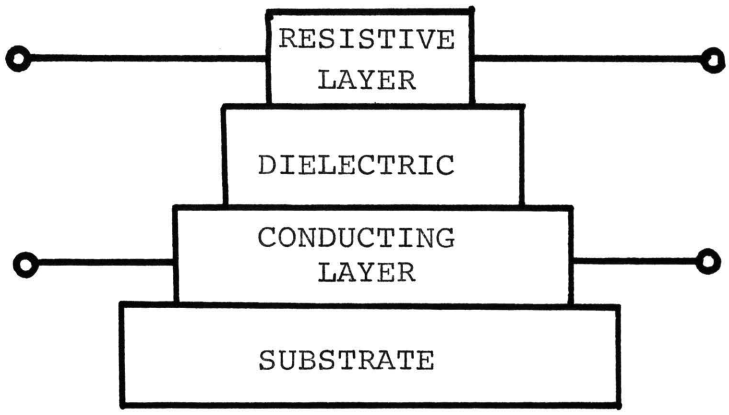

Figure 3. A Thin-Film $\overline{\text{URC}}$

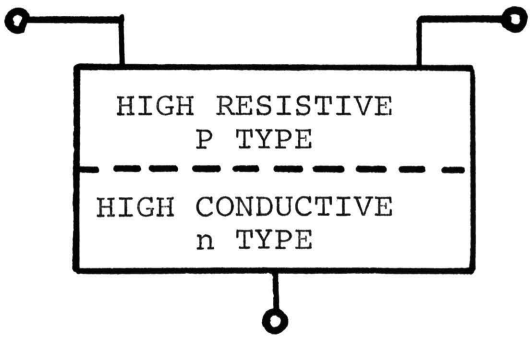

Figure 4. A pn Junction Distributed Network

one side made of a material with high resistivity and the other side made of a high-conductivity material. The high-conductivity side serves as a common short circuit, and the high-resistivity layer serves as the distributed resistance. Distributed capacitance comes from the junction capacitance of the revese-biased junction.

B. STATE-VARIABLE SYNTHESIS OF DISTRIBUTED RC NETWORKS

1. Extended State-Variable Synthesis

Consider the lumped scalar transfer function given in equation (2.6).

$$T(s) = \frac{N(s)}{D(s)} = d + \frac{b_{n-1}s^{n-1} + \ldots + b_1 s + b_o}{s^n + a_{n-1}s^{n-1} + \ldots + a_o} \qquad (2.6)$$

T(s) may be realized by the block diagram shown in Figure 5. The summing junctions and 1/s blocks are standard operational amplifier circuits [10].

Now consider the transfer function described by equation (2.7), where F(s) is any scalar function of s.

$$T(s) = T(F(s)) = d + \frac{b_{n-1}F^{n-1}(s) + b_{n-2}F^{n-2}(s) + \ldots + b_1 F(s) + b_o}{F^n(s) + a_{n-1}F^{n-1}(n) + \ldots + a_o} \qquad (2.7)$$

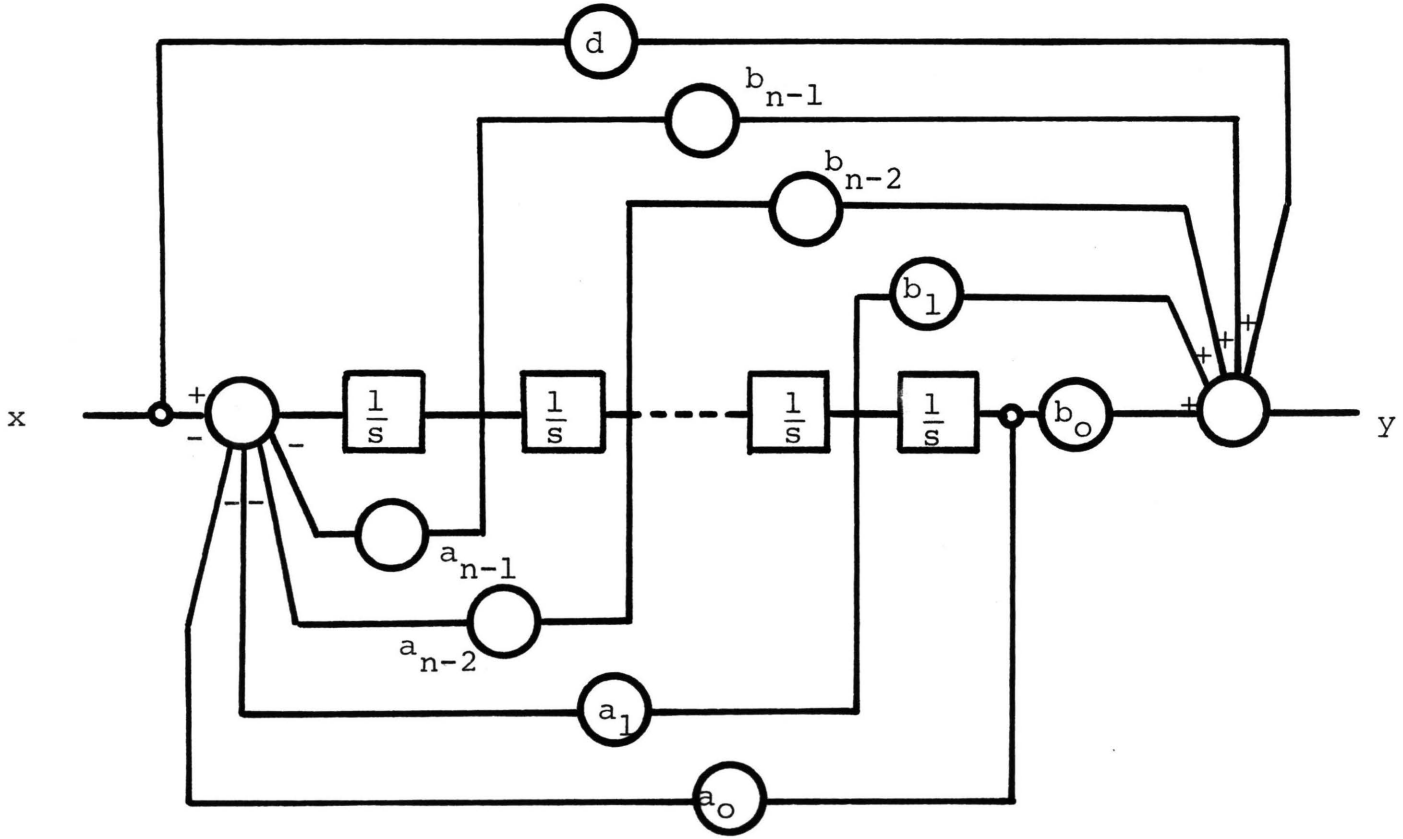

Figure 5. Block Diagram Realization of Equation (2.6)

Equation (2.7) may be realized by the block diagram of Figure 6. It should be noted that the only difference between this diagram and the diagram of Figure 5 is that the 1/s blocks have been replaced by 1/F(s) "integrators".

Kozemchak (p. 151) refers to this as extended state-variable synthesis, and he presents the following theorem [3].

Let F=F(s) be any function of the Laplace variable s. The necessary and sufficient condition for T(F)=N(F)/D(F) to be realizable by this extended state-variable procedure is that 1/F(s) be the transfer function of a realizable network.

It follows that since no restrictions are placed on F(s), F(s) can be hyperbolic or exponential function of $\sqrt{s}$. As has been stated before, distributed RC networks are characterized by such functions; thus, the extended state-variable procedure can be used for synthesis of distributed RC networks.

2. Integrators for Extended State-Variable Synthesis

Three main transformations have been used in the synthesis of distributed RC networks. These are [6,12,13]:

$$\lambda = \tanh \sqrt{sRC} \qquad (2.8a)$$

$$P = \cosh \sqrt{sRC} \qquad (2.8b)$$

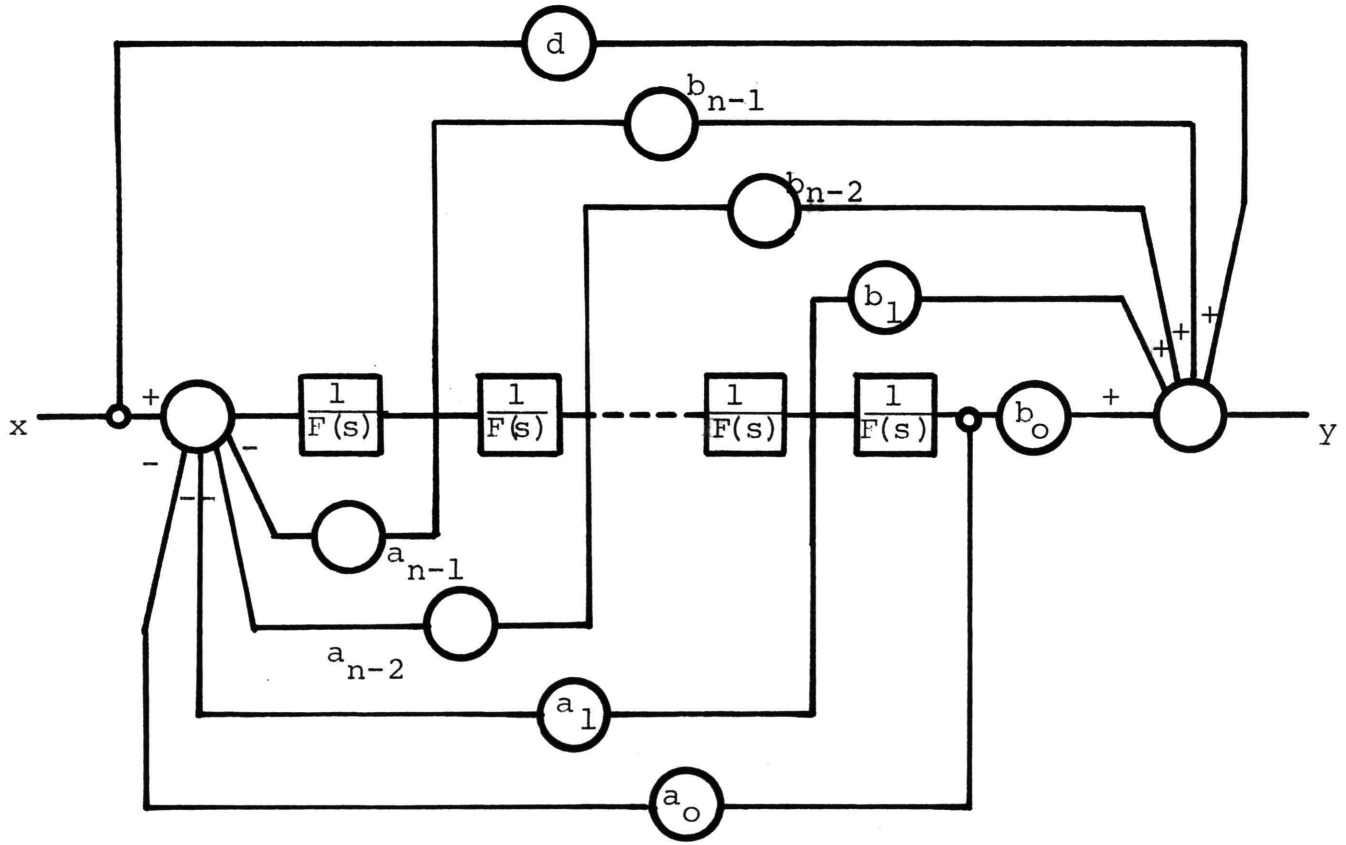

Figure 6. Block Diagram Realization of Equation (2.7)

$$w = \exp \sqrt{sRC}. \tag{2.8c}$$

"Integrators" for the extended state-variable syntheses have been developed using each of these transformations [3,14]. These are shown in Figure 7. The derivations of the transfer functions for each of these circuits may be summarized as follows:

For Figure 7a (λ-plane integrator)

$$\frac{V_2(s)}{V_1(s)} = -\frac{zf(s)}{zi(s)} = \frac{z_o}{\frac{\sqrt{s}\ \tanh \sqrt{sRC}}{1}\ z_o} = \frac{1}{\tanh \sqrt{sRC}} = \frac{1}{\lambda} \tag{2.9a}$$

where $z_o = \sqrt{\frac{R}{sC}}$.

For Figure 7b (P-plane integrator)

$$\frac{V_2(s)}{V_1(s)} = \frac{V_2(s)}{V_1(s)}\bigg|_{I_2=0} = \frac{z_{21}}{z_{11}} = \frac{\operatorname{csch} \sqrt{RCs}}{\coth \sqrt{RCs}} = \frac{1}{\cosh \sqrt{RCs}} = \frac{1}{P}. \tag{2.9b}$$

For Figure 7c (w-plane integrator)

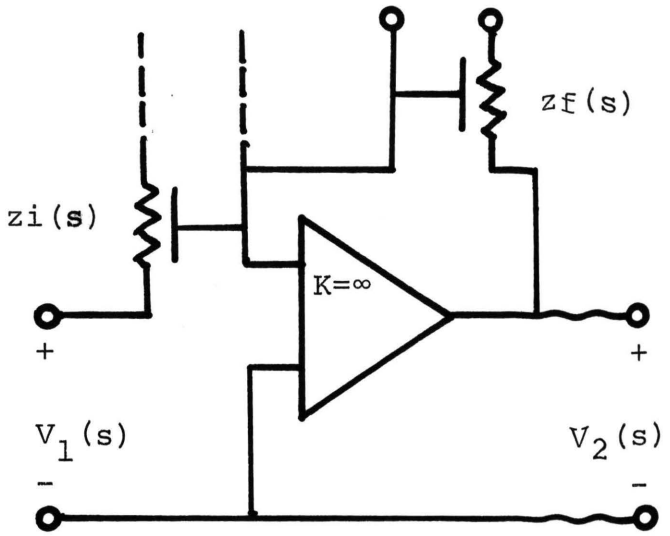

(a)

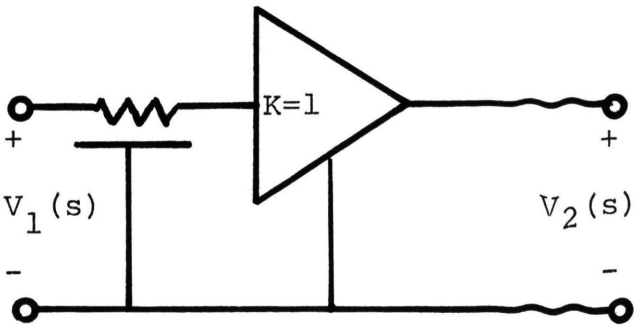

(b)

Figure 7. Integrators for Extended State-Variable Synthesis (continued)

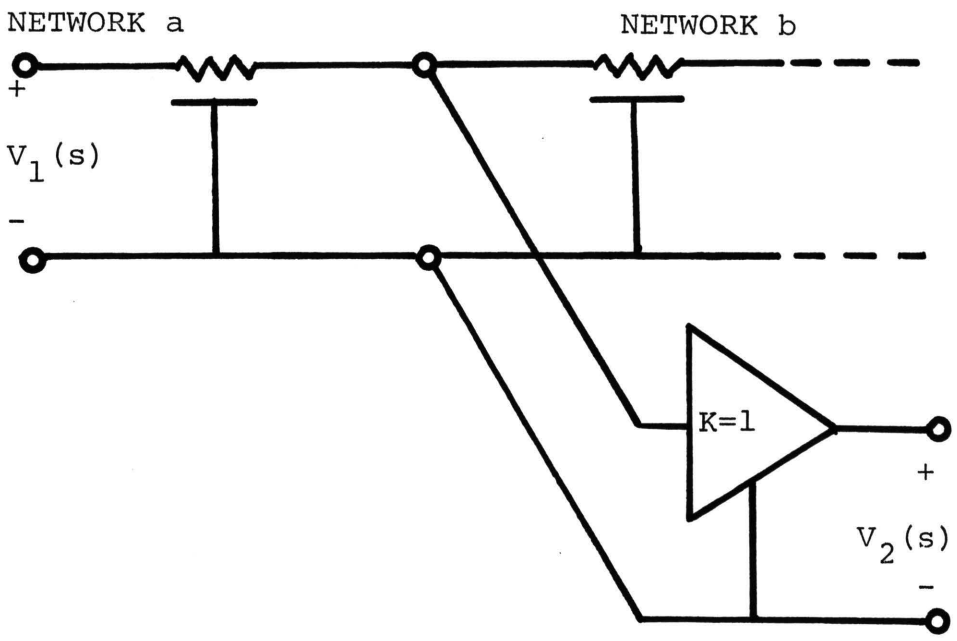

(c)

Figure 7. Integrators for Extended State-Variable Synthesis

$$\frac{V_2(s)}{V_1(s)} = \frac{-Y_{21a}}{Y_{22a} + \frac{1}{z_{11b}}} = \frac{\cosh \sqrt{R_b C_b s}}{\cosh (\sqrt{R_a C_a s} + \sqrt{R_b C_b s})}$$

$$= \frac{e^{-\sqrt{R_a C_a s}} (1 + e^{-2\sqrt{R_b C_b s}})}{1 + e^{-2(\sqrt{R_b C_b s} + \sqrt{R_a C_a s})}}$$

$$\simeq e^{-\sqrt{R_a C_a s}} = \frac{1}{w} \qquad (2.9c)$$

where $\frac{C_a}{R_a} = \frac{C_b}{R_b}$ and $R_b C_b >> R_a C_a$.

The λ and w-plane "integrators" require an infinite length line for an exact realization. This is not intolerable, however, since the RC line is dissipative. A relatively long line will be sufficient to approximate an infinite length line to a fair degree of accuracy [3, 14].

In summary, "integrators" for the extended state-variable synthesis of distributed RC networks exist and use three of the most common transformations found in the literature.

3. Stability of Distributed RC Network Transfer Functions

Although the extended state-variable synthesis allows transfer functions to contain poles anywhere in the transformed planes, it has been found that stable transfer functions contain poles only in certain regions of the transformed planes. The stable regions for each of the three transformed planes are shown in Figure 8 [3,12,13].

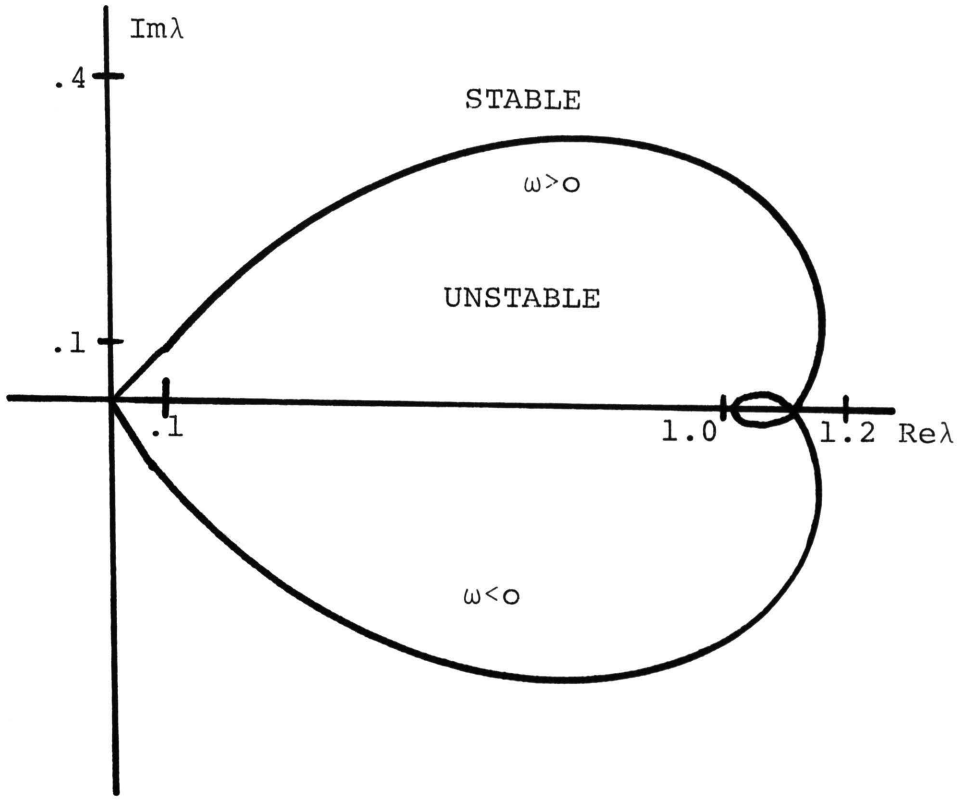

(a)

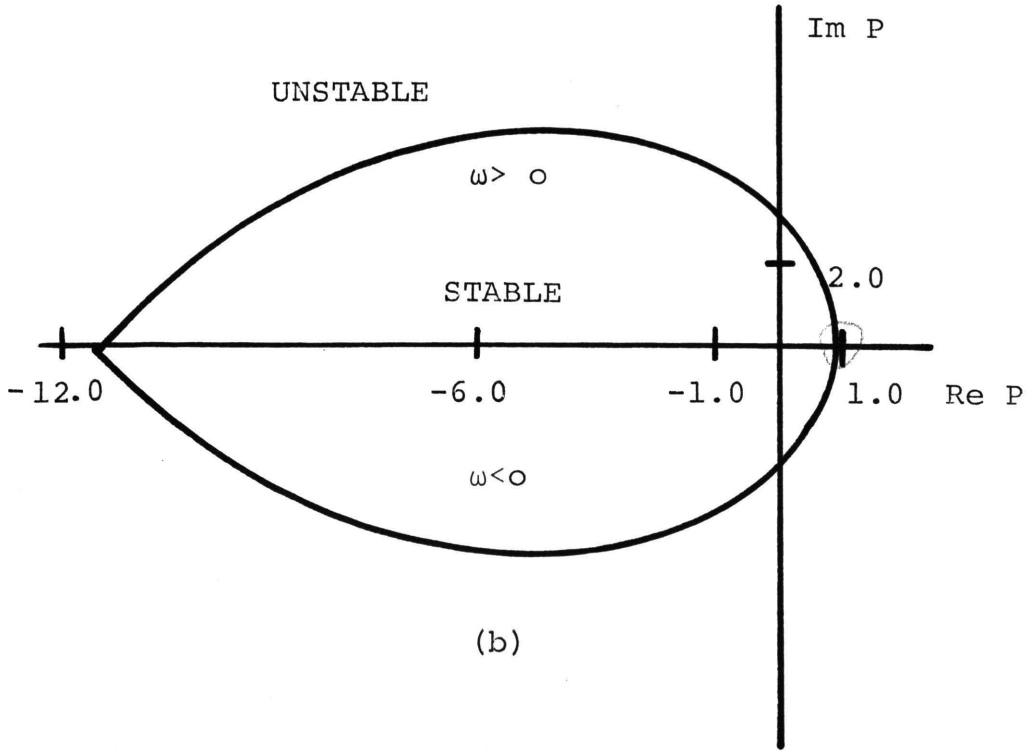

(b)

Figure 8. Stable Regions for the λ, P, and w-planes (continued)

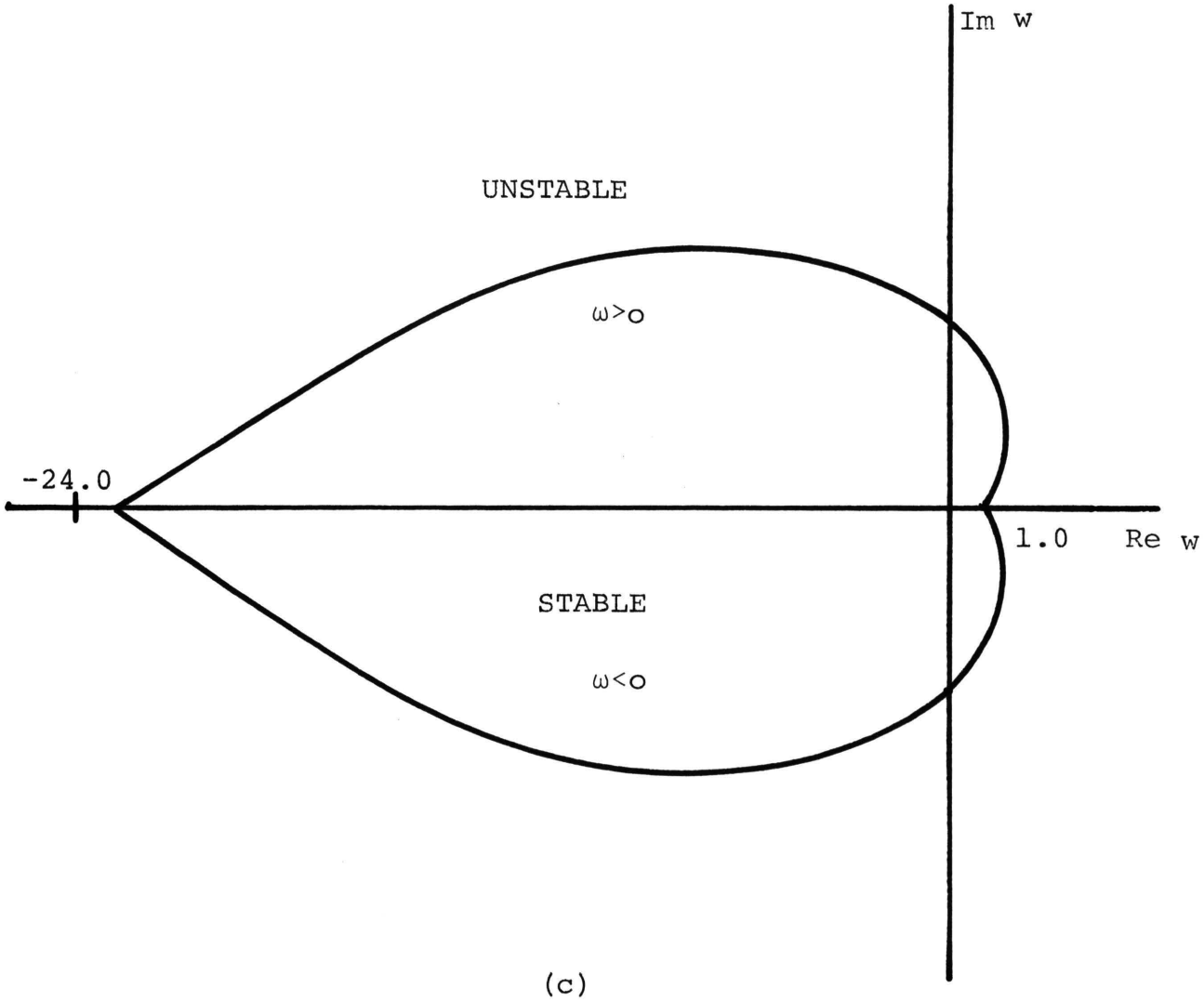

Figure 8. Stable Regions for the λ, P, and w-planes

III. THE APPROXIMATION PROBLEM

A. FORMULATION OF AN ERROR EXPRESSION

For the purposes of this paper error is defined to be

Error=(Desired specification)-(Actual realization). (3.1)

An often-used error expression is the integral squared error (I.S.E.) [15]. In this error expression equation (3.1) is squared and integrated over all frequencies. The resulting expression is

$$\text{I.S.E.} = \int_0^\infty (\text{Error})^2 \, d\omega. \tag{3.2}$$

If the desired magnitude function is defined as $G(\omega)$, and the actual realization is a distributed RC network transfer function, $T(s)$, then equation (3.2) becomes

$$\text{I.S.E.} = \int_0^\infty [G(\omega) - |T(j\omega)|]^2 \, d\omega \tag{3.3}$$

where $|T(j\omega)|$ denotes the magnitude of the transfer function, $T(s)$, at $s=j\omega$. It is often desirable to add a weighting function, F, to the error expression to penalize some frequencies more than others. The general error expression

becomes

$$\text{I.S.E.} = \int_0^\infty F[G(\omega) - |T(j\omega)|]^2 \, d\omega. \qquad (3.4)$$

The approximation procedure is then to start with a particular T(s) of a known form, such as in equation (2.7), but with unknown coefficients, a_i and b_i. Numerical optimization techniques are then used to find the coefficients of T(s) that give the smallest I.S.E. The only constraint on the a_i and b_i is that they do not cause a pole of T(s) to be outside the stability regions shown in Figure 8. Since equation (3.4) involves an expression containing the magnitude of a transfer function, the I.S.E. will almost always be impossible to evaluate analytically; fortunately this integral may be accurately approximated by numerical methods [16].

B. USE OF THE TECHNIQUE TO APPROXIMATE AN IDEAL LOW-PASS FREQUENCY RESPONSE

Now consider the curve given in Figure 9. This is an ideal low-pass filter response, and the G(ω) of equation (3.4) may be written as

$$\begin{aligned} G(\omega) &= 1 \qquad 0 \leq \omega \leq \omega_o \\ G(\omega) &= 0 \qquad \omega > \omega_o \quad . \end{aligned} \qquad (3.5)$$

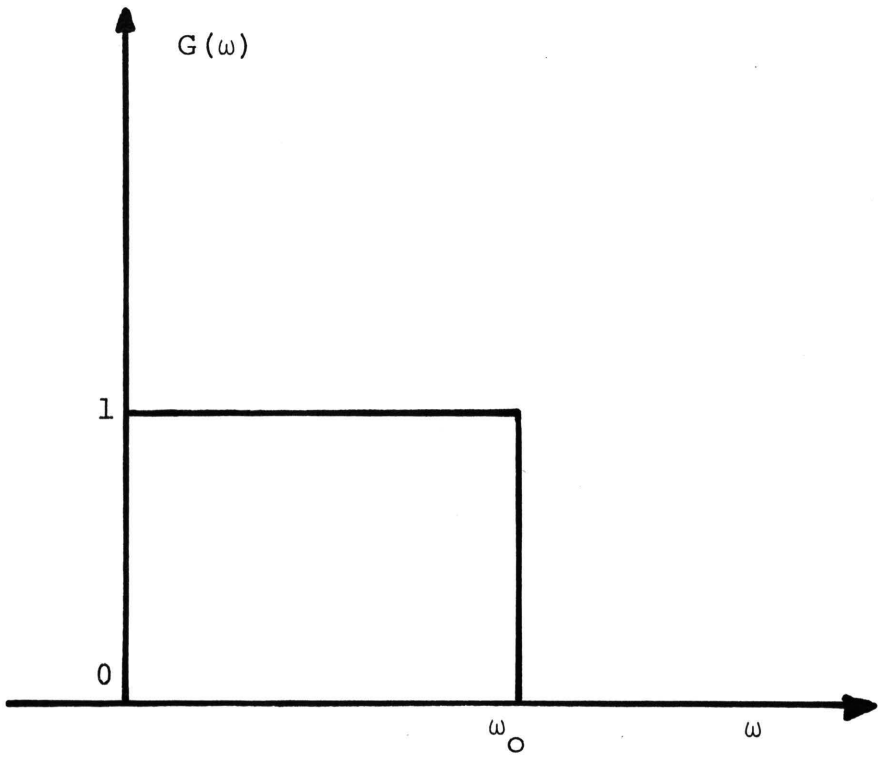

Figure 9. Frequency Response of an Ideal Low-Pass Filter

It can be shown that this response is impossible to obtain exactly [17]. Although it is impossible to attain exactly, Figure 9 is an excellent ideal specification to approximate using the method described above.

First, equation (3.4) is rewritten for the $G(\omega)$ of equation (3.5) as

$$I.S.E. = \int_{o}^{\omega_o} F[1-\left|T(j\omega)\right|^2]\, d\omega + \int_{\omega_o}^{\infty} F\left|T(j\omega)\right|^2\, d\omega. \qquad (3.6)$$

Previous results have shown that distributed RC transfer functions of the form

$$T_1(P(s)) = \frac{K_1}{P^n + a_{n-1}P^{n-1} + \ldots + a_1 P + a_o} \qquad (3.7a)$$

$$T_2(w(s)) = \frac{K_2}{w^m + b_{m-1}w^{m-1} + \ldots + b_1 w + b_o} \qquad (3.7b)$$

where K_1 and K_2 are real constants, have frequency responses that approximate Figure 9 [7,8]. The λ-plane is not well suited for low-pass approximation. Both T_1 and T_2 can easily be realized by the extended state-variable synthesis technique. For each computer run n or m is fixed, and the resulting

output contains the values of the a_i or b_i that give the smallest I.S.E. without placing poles of the transfer function outside of the stability regions shown in Figure 8. ω_o is taken as the 3db frequency.

To insure that the minimum I.S.E. is obtained ω_o is not fixed. If ω_o were fixed, the a_i or b_i that give a minimum I.S.E. for that particular ω_o would be obtained, but the possibility would exist that with another ω_o another set of a_i or b_i would give an even smaller I.S.E. Thus, ω_o is calculated for each set of a_i or b_i obtained in the optimization process.

Unfortunately, another problem arises when ω_o is allowed to vary. Since it may be that

$$\lim_{a \to o} \int_o^a f(x)dx = 0, \tag{3.8}$$

a small ω_o might result in a correspondingly small I.S.E., not because $|T(j\omega)|$ is approaching $G(\omega)$, but because the upper limit on the first integral of equation (3.6) is approaching zero. To avoid this problem the weighting function F is defined to be

$$F = \frac{\omega_o^2 + 100}{\omega_o^2} \tag{3.9}$$

and thus can be placed outside the integrals of equation (3.6). This serves to penalize low values of ω_o. This does

not interfere with the approximation process, since transfer functions with low ω_o are usually poor approximations of the ideal response [7,8].

Finally to facilitate a solution by numerical methods, the infinite limit on the second integral in equation (3.6) is changed to 100 ω_o.* Thus, the I.S.E. expression for the low-pass filter approximation becomes

$$\text{I.S.E.} \simeq \frac{100+\omega_o^2}{\omega_o^2}\left[\int_o^{\omega_o}\left[1-|T(j\omega)|^2 d\omega+\int_{\omega_o}^{100\omega_o}|T(j\omega)|^2 d\omega\right]\right. . \quad (3.10)$$

With the error expressed in this way the problem has now been reduced to a typical non-linear programming problem, and various computer routines have been written to solve such problems [18].

A block diagram of the computer program used to find the minimum I.S.E. is shown in Figure 10. The particular T(s) must be entered as well as an initial estimate of the coefficients. A Newton-Raphson technique is used to find the cutoff frequency. The value of ω_o is then placed into equation (3.10), the integrals of which are numerically evaluated by a 32-point Gaussian quadrature formula. The resulting value of I.S.E. is stored in the optimization routine, a new set of coefficients are generated, and the I.S.E. is again computed. This value is compared with the previous value of I.S.E., and from the difference of these two values a corresponding change in the coefficients is

*See appendix

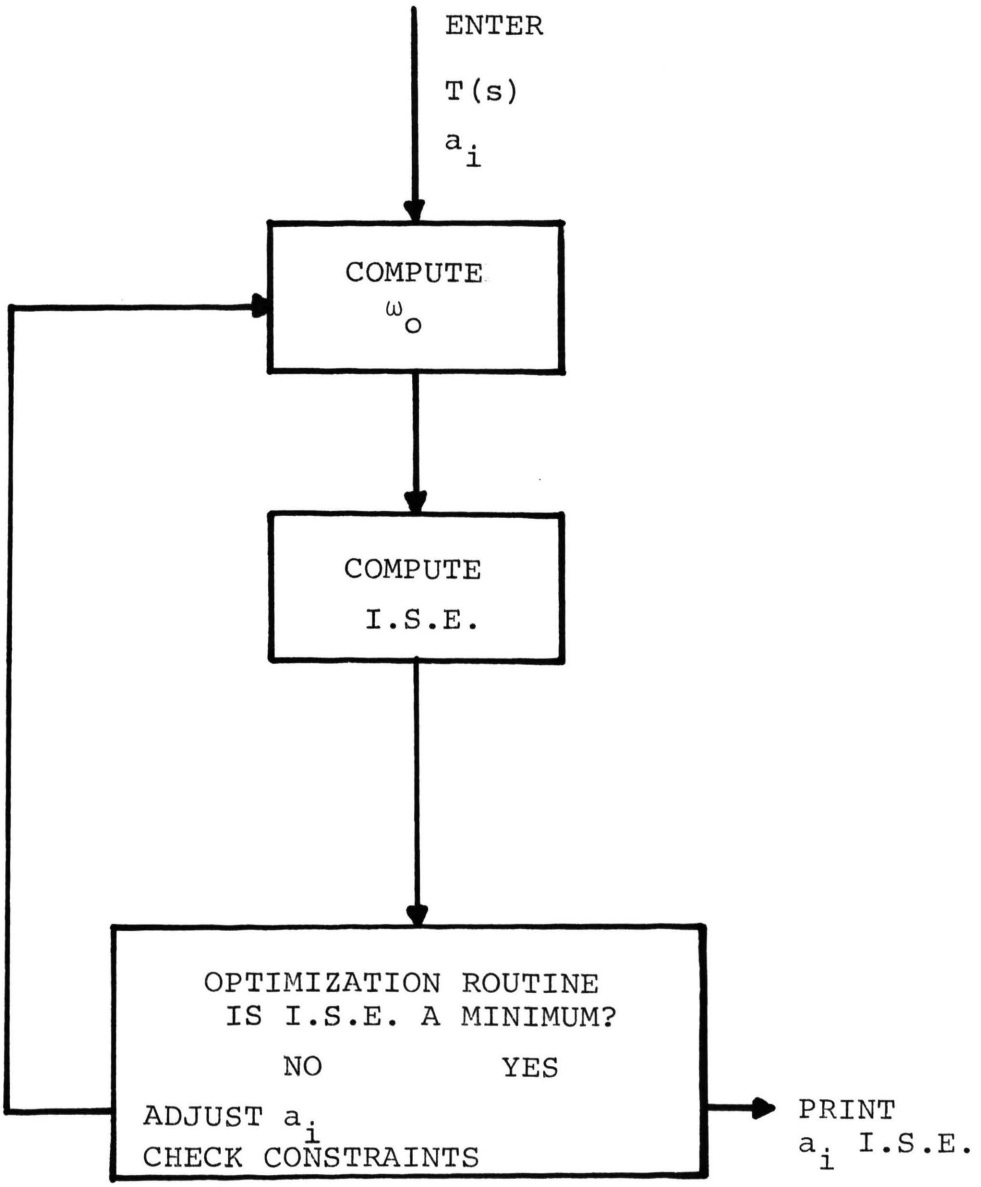

Figure 10. Block Diagram of Computer Routine

made; the process is repeated until a minimum I.S.E. is obtained.

Both a gradient technique and a direct-search technique were used for the optimization routine, and both worked equally well. This suggests that any optimization routine should work.

The procedure described above was used on first-second-third-and fourth-order P-plane transfer functions and on first-second-and third-order w-plane transfer functions. The resulting frequency-response curves are shown in Figures 11 and 12. These curves show that a first-order P-plane filter has a high frequency roll-off rate that is exponentially increasing with a minimum value of approximately $\frac{-44dB}{Decade}$ which is greater than a second-order lumped filter. Similarly a second-order P-plane filter has a minimum roll-off rate of $\frac{-114\ dB}{Decade}$ which is greater than a fifth-order lumped filter. Further increases in the order result in correspondingly sharper roll-off rates. The high-frequency roll-off rates for the w-plane filters are approximately the same as those for the P-plane filters but the w-plane filters have slightly more ripple in the passband than the P-plane filters.

Table I contains the coefficients of the optimum low-pass transfer functions, and Table II gives the pole locations of these transfer functions. It should be noted here that throughout this discussion the RC product of the distributed

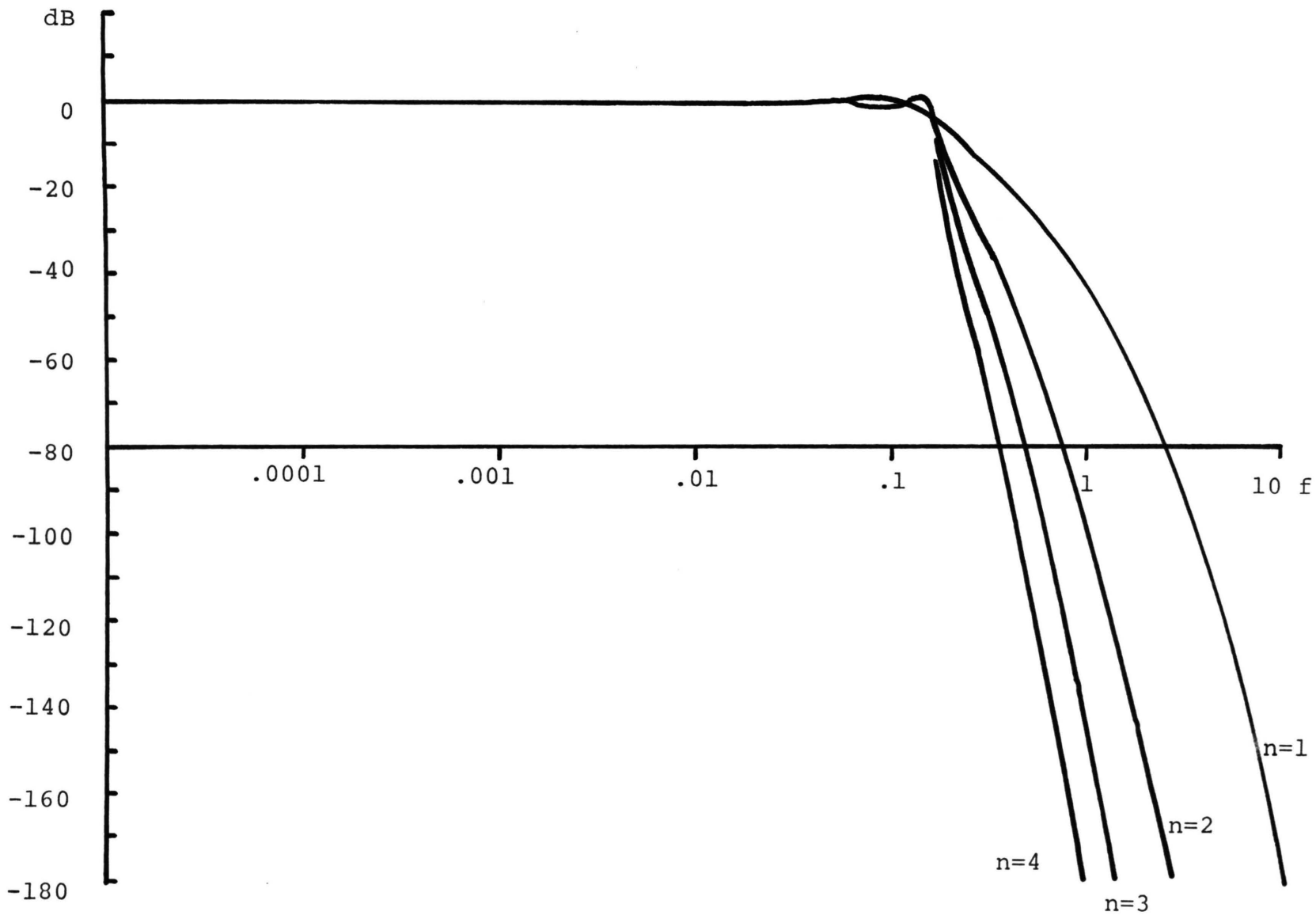

Figure 11. P-plane Frequency Responses

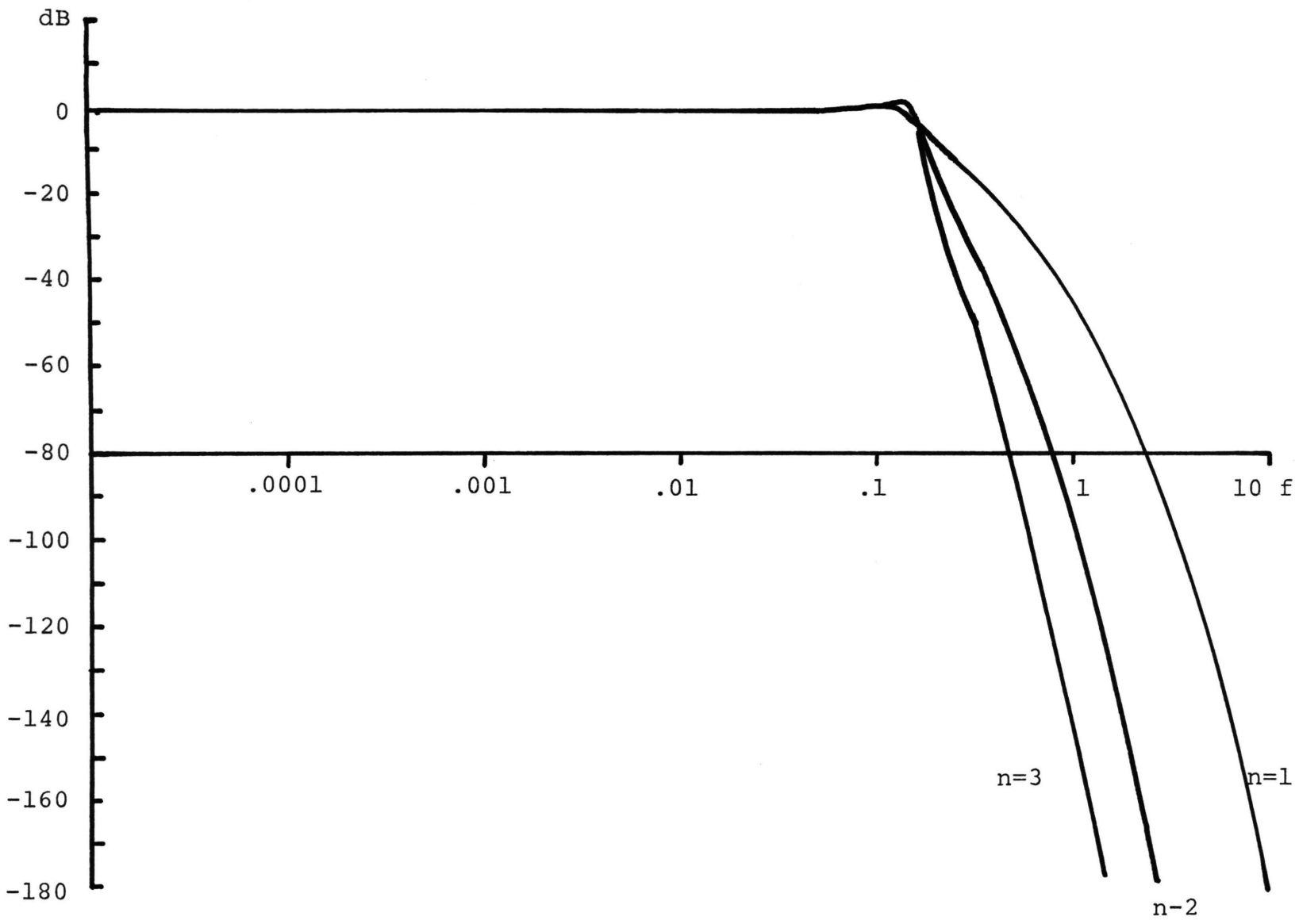

Figure 12. w-plane Frequency Responses

$$\text{For } T(s) = \frac{K}{P^n + a_{n-1} P^{n-1} + \ldots + a_1 P + a_o}$$

$$\text{or } T(s) = \frac{K}{w^n + a_{n-1} w^{n-1} + \ldots + a_1 w + a_o}$$

TABLE I. COEFFICIENTS OF P-AND w-PLANE LOW-PASS TRANSFER FUNCTIONS

	n	RC for ω_o=1	a_3	a_2	a_1	a_o
P-plane	1	15.6	--	--	--	2.92
	2	19.0	--	--	9.21	11.38
	3	19.2	--	13.98	48.78	41.9
	4	19.27	27.41	262.6	1013.0	1287.0
w-plane	1	16.97	--	--	--	7.16
	2	18.84	--	--	19.12	62.1
	3	19.22	--	29.16	228.8	542.9

TABLE II. POLES OF P-AND w-PLANE LOW-PASS TRANSFER FUNCTION

	n	POLES
P-plane	1	-2.92
	2	-1.47, -7.74
	3	-1.29, -3.54, -9.14
	4	-1.09, -2.55, -5.35, -9.80
w-plane	1	-7.16
	2	-4.15, -14.98
	3	-5.43, -5.48, -18.25

network has been normalized to 1. Frequency scaling is done by adjusting the RC product. To aid in scaling, Table I also includes the value of RC required to make ω_o=1. Thus, for example, if it were desired to make the cutoff frequency of a first order P-plane filter equal to 1 kHz, it is first determined that

$$\omega_o = 2\pi f_o$$

$$= 6.28 \times 10^3 \text{ radians/second.} \tag{3.11}$$

Now from Table I

$$RC\ \omega_o = 15.6 \tag{3.12}$$

or

$$RC = \frac{15.6}{\omega_o} \tag{3.13}$$

$$= \frac{15.6}{6.28 \times 10^3} \tag{3.14}$$

so finally,

$$RC = 2.48 \times 10^{-3} \text{ seconds} \tag{3.15}$$

for a cutoff frequency of 1 kHz.

No attempt is made to optimize the phase response of the filters, and as a result, the phase response has no

particularly advantageous characterisitcs. The phase angle increases monotonically with frequency at a rate proportional to the order of the transfer function as shown in Figures 13 and 14 for the P and w-planes, respectively.

C. COMPARISON WITH PREVIOUS TECHNIQUES

For a comparison with previous methods of solution a second-order transfer function is taken as a representative example. The curves of Figure 15 show the results obtained by the three techniques discussed in the introduction. Curve 1 shows the dominant-pole approach which matches the frequency response of the distributed RC transfer function to a lumped transfer function--in this case a fourth order Butterworth [4]. Curves 2 and 3 show frequency responses of second-order P-plane and w-plane transfer functions, respectively, that were picked from available curves [7,8]. Curves 4 and 5 are, respectively, the optimized second-order P-and w-plane low pass frequency responses.

Examination of the curves reveals that the optimized frequency responses are better than those obtained by the other two methods and that the optimized P-plane response (Curve 4) is the best. This conclusion can also be drawn from Table III, which contains the I.S.E. of all five of the curves shown in Figure 15.

In conclusion, barring other considerations such as sensitivity or ease of fabrication, it appears that the

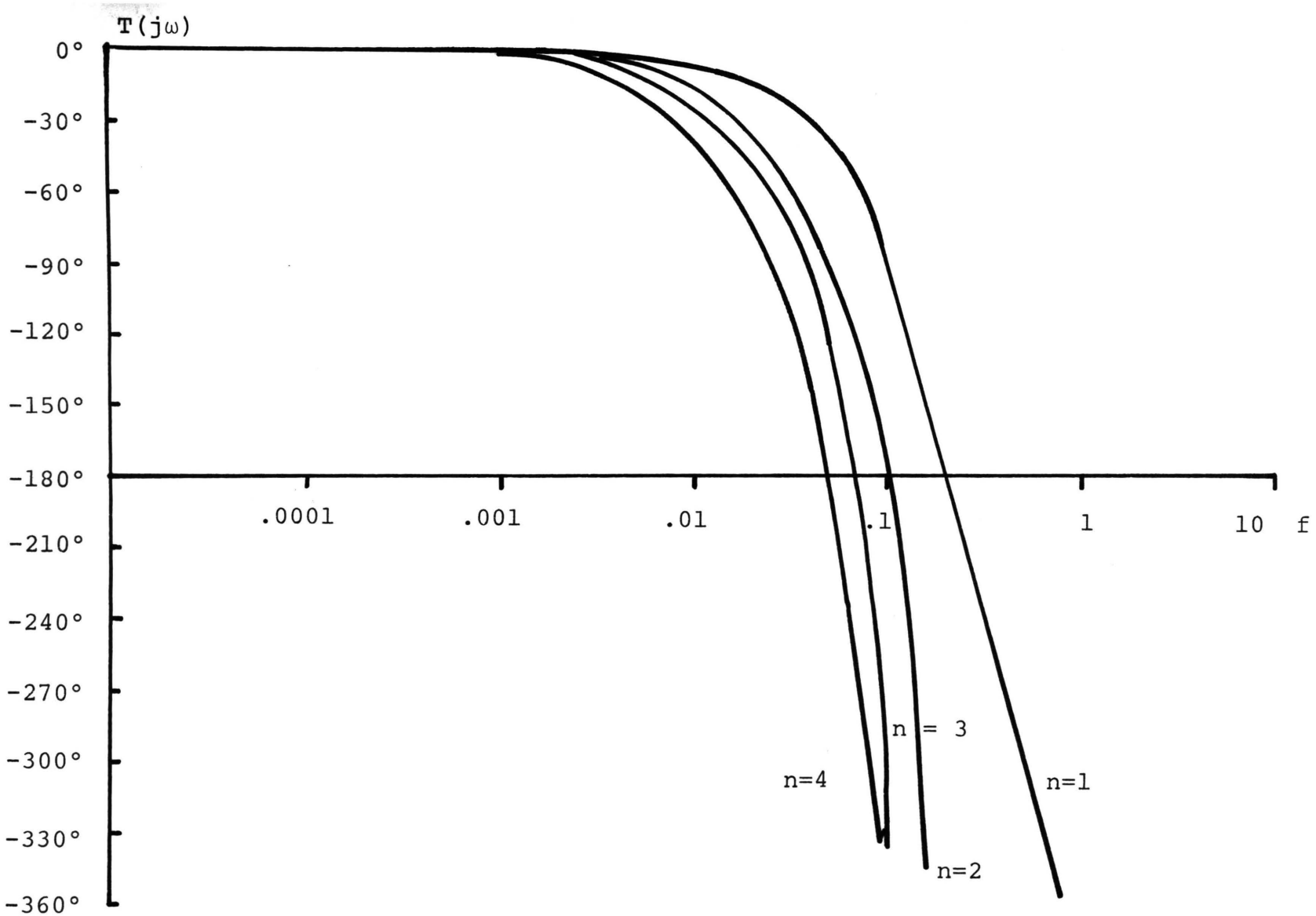

Figure 13. Phase Response of P-plane Transfer Functions

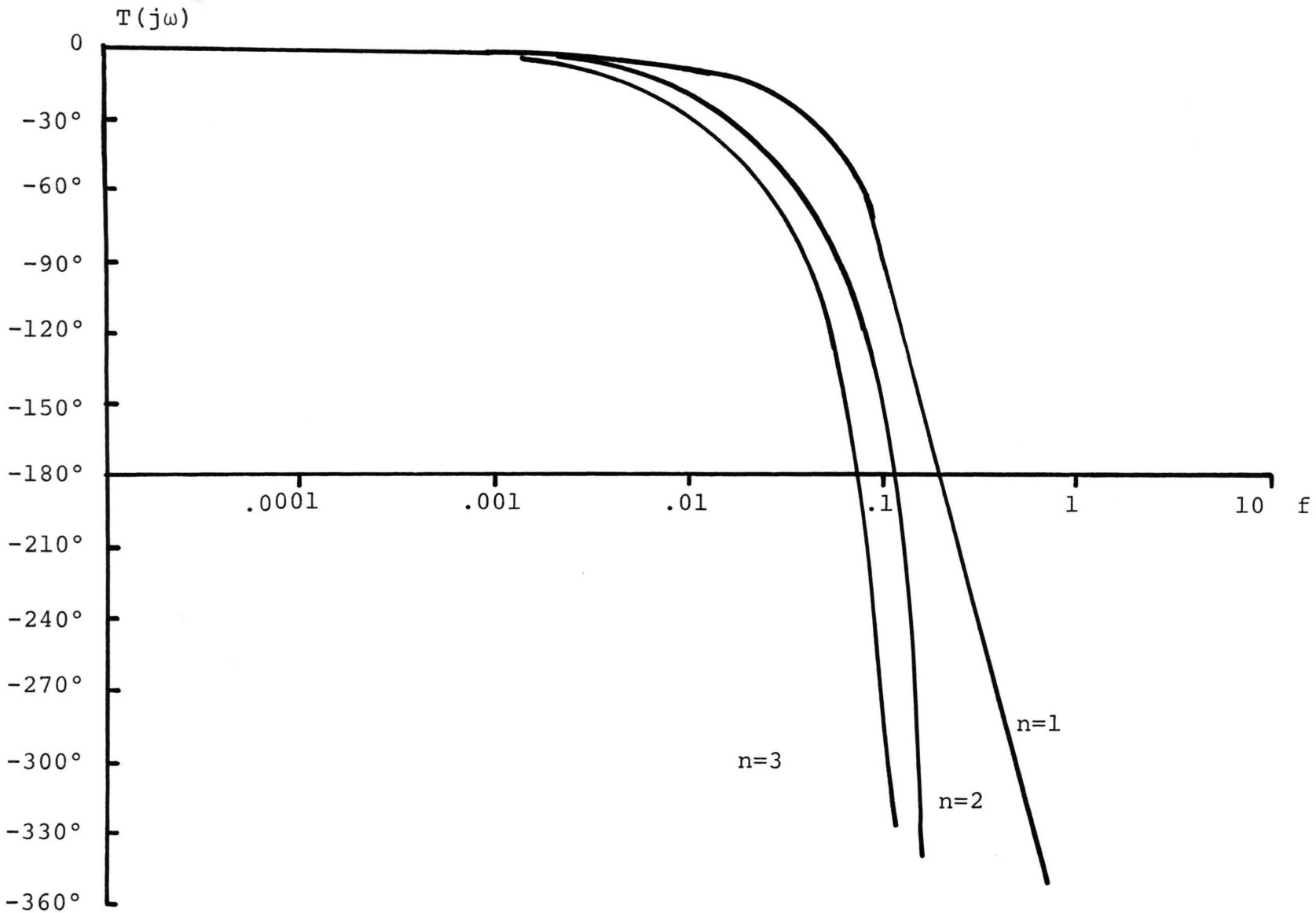

Figure 14. Phase Response of w-plane Transfer Functions

optimized P-plane transfer function produces the "best" approximation to the ideal low-pass frequency response.

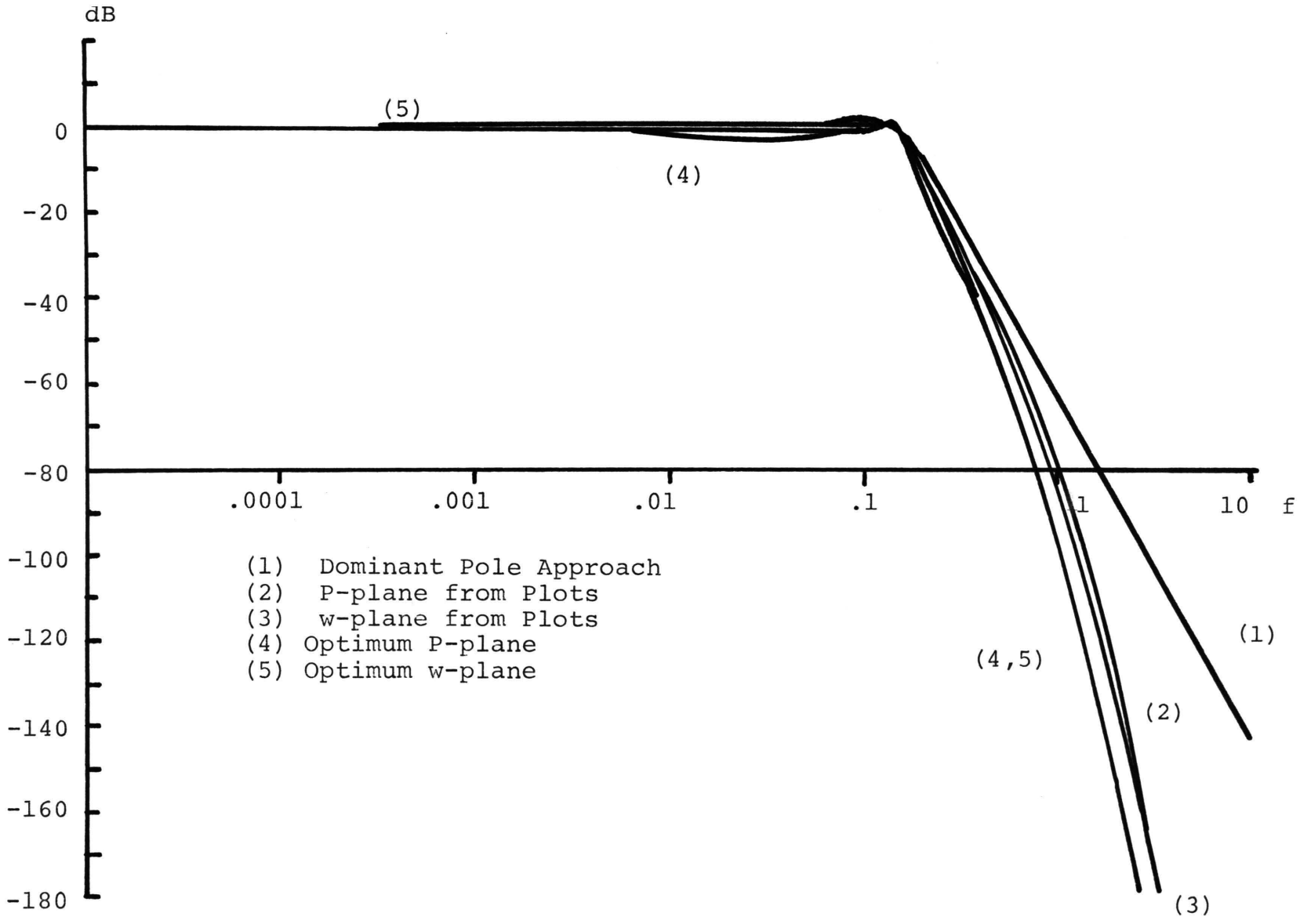

Figure 15. Comparison of Various Responses

TABLE III. I.S.E.'S OF THE CURVES OF FIGURE 15

CURVE	I.S.E.
1	11.15
2	10.79
3	9.17
4	4.18
5	5.48

IV. DESIGN EXAMPLE

Consider the following design example:

Design a low-pass filter with a 3-db cutoff-frequency of 3.92 kHz and with at least 30 db of attenuation at 7.84 kHz. The first step is to normalize the cutoff frequency to $\omega_o=1$. After normalization an inspection of Figure 11 reveals that a second-order P-plane filter meets the design specifications. By consulting Table I the second-order P-plane transfer function is found to be:

$$\frac{V_2(s)}{V_1(s)} = \frac{K}{P^2 + 9.21\ P + 11.38},\ RC = 19.0 \qquad (4.1)$$

where K is an arbitrary gain constant.

The block diagram of this transfer function is shown in Figure 16. Straight-foreward synthesis techniques are then used to obtain the circuit of Figure 17 [10]. K is chosen to be approximately 2158 which gives a dc gain of 20 db. Amplifier A4 is used to provide this gain; it may be removed without affecting the filter performance. Thus, the actual filter consists of only three operational amplifiers, six lumped resistors and two distributed RC networks. All the resistors are within the range of 100 Ω to 30 KΩ, which is the most typical range for integrated circuits [19].

Frequency scaling is done as illustrated in Chapter 3. In this case

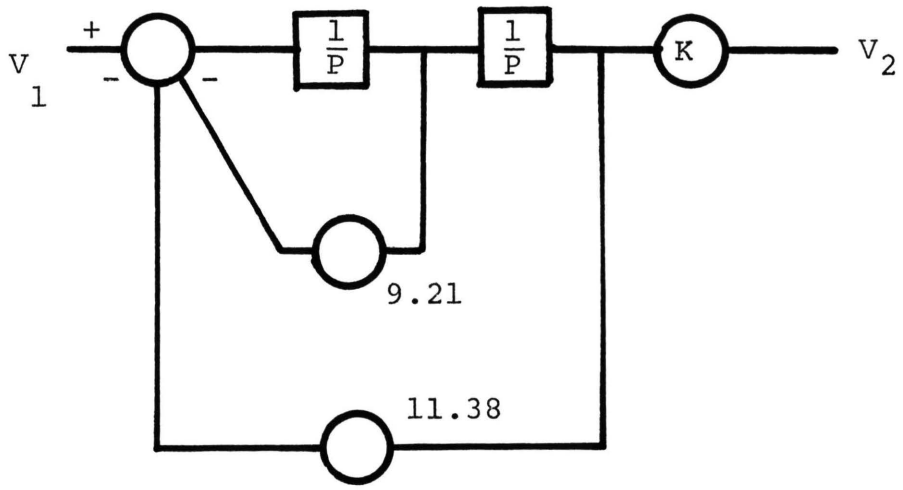

Figure 16. Block Diagram Realization of Equation (4.1)

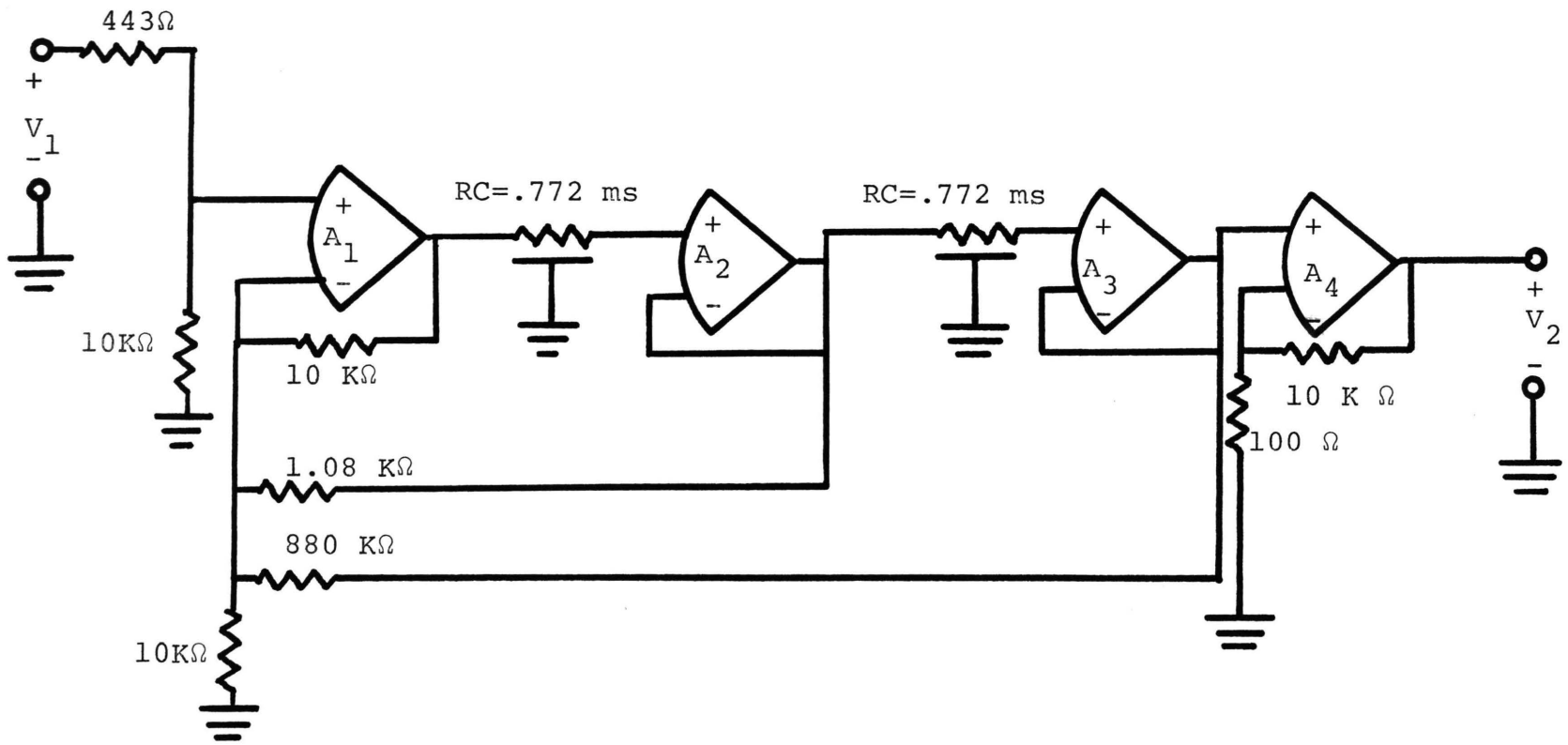

Figure 17. Circuit Diagram for Second Order P-Plane Low-Pass Filter

$$RC\ \omega_o = 19.0 \tag{4.2}$$

$$RC = \frac{19.0}{24.6 \times 10^3} = 0.772 \text{ msec.} \tag{4.3}$$

This time constant may be realized by making R=27.6 KΩ and C = 0.028 μf.

Figure 18 shows the frequency response of the circuit of Figure 17 taken from actual laboratory data compared with the theoretical frequency response of equation (4.1). The two curves show good agreement in most places with slight differences that can be attributed to stray effects in the circuit. These differences can possibly be decreased by adjusting the circuit components. Thus, it is demonstrated that the extended state-variable synthesis of the optimum transfer function yields a circuit that performs very close to the theoretical expectations and that is capable of being completely integrated.

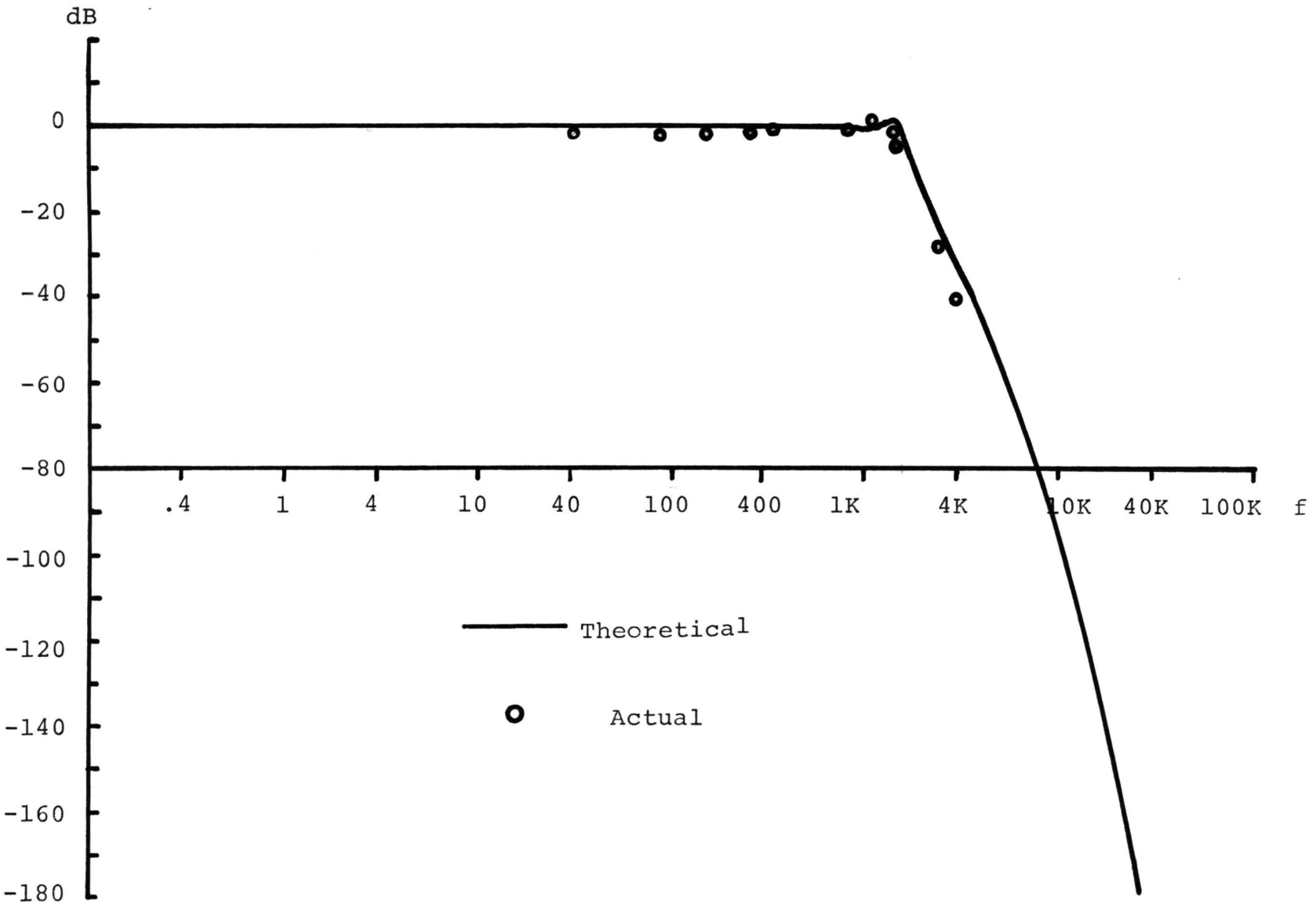

Figure 18. Comparison of Actual and Theoretical Frequency Responses of Second-order P-plane Low-Pass Filter

V. CONCLUSIONS AND RECOMMENDATIONS

The simplicity and versatility of the extended state-variable synthesis technique for distributed RC networks suggests an equally simple and versatile solution to the approximation problem. An error expression is formulated in Chapter 3 for any desired response. Using numerical optimization techniques to minimize the error, a set of design tables are constructed that not only simplify the approximation problem, but also produce approximations that are superior to those obtained by other methods. Chapter 4 shows the practicality of the entire process by constructing a working circuit from the theoretical data.

A comparison of the P-plane and w-plane realizations of the low-pass filter indicate that the P-plane realization is more successful in approximating the ideal low-pass frequency response. The P-plane "integrator" is also easier to fabricate.

The only disadvantage of this approximation procedure is that the optimum values obtained are only optimum because they satisfy the error expression derived in Chapter 3. Another error expression undoubtedly produces another set of optimum values. In short, there are as many optimum solutions, as there are error expressions. The user must carefully consider which set of optimum values is best for the particular application. Thus, the solution obtained in this paper is not intended to be the final solution to

the low-pass approximation problem for distributed RC networks. But at present the values obtained here are the only ones available. They can serve as a "general-purpose" set of coefficients until more insight into the problem is obtained and new error expressions and corresponding optimum values for more specific applications are produced.

The obvious extension of the present research would be in the determination of the transfer functions of optimum high-pass and band-pass active distributed RC filters. The procedures would be similar to those used for the low-pass case.

Other topics for further research would be sensitivity studies of the distributed RC transfer functions. A comparison of the sensitivities of a P-plane and a w-plane transfer function would be informative. Another possible research topic would be the investigation of the use of tapered distributed RC networks in the synthesis. An optimization of both the taper and the coefficients of the transfer function may produce better approximations.

BIBLIOGRAPHY

1. KERWIN, W. J., Analysis and Syntheses of Active RC Networks Containing Distributed and Lumped Elements, Ph.D. Dissertation, Stanford University, August 1967.

2. LIN, H. C., Integrated Electronics, Holden-Day, 1967.

3. KOZEMCHAK, E. B., State Variable Synthesis of Distributed RC Network Transfer Function, in Papers on Integrated Circuit Synthesis, II, compiled by R. Newcomb and R. de Oliveira, Stanford Electronics Laboratories, Technical Report No. 6560-13, June 1967.

4. BELLO, V. G., and GHAUSI, M.S., Active Distributed RC Realization of Low-Pass Magnitude Specifications, IEEE Transactions on Circuit Theory, Vol. CT-16, August 1969.

5. BELLO, V. G., and GHAUSI, M.S., Design of Linear Phase Active Distributed RC Networks, IEEE Transactions on Circuit Theory, Vol. CT-16, November 1969.

6. WYNDRUM, R. W., Jr., The Exact Synthesis of Distributed RC Networks, Technical Report 400-76, College of Engineering, New York University, May 1963.

7. BARRON, M. B., Synthesis of Distributed RC Networks, in Papers on Integrated Circuit Synthesis, compiled by R. W. Newcomb and T. N. Rao, Stanford Electronics Laboratories, Technical Report No. 6560-4, June 1966.

8. WEN, C. M., A Synthesis Procedure of Distributed RC Parameter Networks, UMR Master's Thesis, 1969.

9. HERSKOWITZ, G. J., Computer-Aided Integrated Circuit Design, McGraw-Hill, 1968.

10. NEWCOMB, R. W., Active Integrated Circuit Synthesis, Prentice Hall, 1968.

11. GHAUSI, M. S., and KELLY, J. J., Introduction to Distributed Parameter Networks, Holt, Rinehart, and Winston, 1968.

12. O'SHEA, R. P., Synthesis Using Distributed RC Networks, IEEE Transactions on Circuit Theory, Vol. CT-12, No. 4, December 1965.

13. BOURQUIN, J. J., Stability of a Class of Lumped Distributed Systems, Coordinate Science Laboratory Report R-273, University of Illinois, 1968.

14. HENSLEY, R. D., Synthesis of Active Distributed RC Networks Via the $w = e^{\sqrt{s}}$ Transformation, UMR Master's Thesis, 1971.

15. YENGST, W. C., Procedures of Modern Network Synthesis, MacMillan, 1964.

16. MC CALLA, T. R., Introduction to Numerical Methods and Fortran Programming, John Wiley, 1967.

17. JAVID, M., and BRENNER, E., Analysis Transmission and Filtering of Signals, McGraw-Hill, 1963.

18. BEVERIDGE, G. S., and SCHECHTER, R. S., Optimization: Theory and Practice, McGraw-Hill, 1970.

19. SCHILLING, D. L., and BELOVE, C., Electronic Circuits: Discrete and Integrated, McGraw-Hill, 1968.

VITA

Robert Iman Egbert was born on May 25, 1950 in St. Louis, Missouri. He received his primary and secondary education in St. Louis and St. Louis County, Missouri. He graduated from Riverview Gardens Senior High School in June 1968 and in September of 1968 he entered the University of Missouri - Rolla, in Rolla, Missouri. In May 1972 he received a Bachelor of Science degree in Electrical Engineering from the University of Missouri - Rolla.

He entered the Graduate School of the University of Missouri - Rolla in September 1972 and has held a Graduate Teaching Assistantship in the Department of Electrical Engineering since that time. He is a member of IEEE, Eta Kappa Nu, Tau Beta Pi, and Phi Kappa Phi.

APPENDIX

JUSTIFICATION OF THE REPLACEMENT OF INFINITY BY 100 ω_o IN EQUATION (3.10)

In equation (3.10) the infinite limit on the integral of equation (3.8) was replaced by 100 ω_o. This change can be justified by showing that the error from 100 ω_o to infinity is small compared with the error from ω_o to 100 ω_o. This is done by finding a lower bound on the error from ω_o to 100 ω_o and finding an upper bound on the error from 100 ω_o to ∞ then proving that the ratio of the upper bound on the error from 100 ω_o to infinity to the lower bound on the error from ω_o to 100 ω_o is considerably less than one.

The first step is to rewrite equation (3.10) with the error term from 100 ω_o to infinity included. Equation (3.10) becomes

$$I.S.E.= \frac{\omega_o^2+100}{\omega_o^2} \left[\int_o^{\omega_o} [1-|T(j\omega)|]^2 d\omega+\int_{\omega_o}^{100\omega_o} |T(j\omega)|^2 d\omega+\int_{100\omega_o}^{\infty} |T(j\omega)|^2 d\omega\right] \tag{A.1}$$

Now proceed to find a lower bound on the error from ω_o to $100\omega_o$. The P-plane transfer functions that are optimized to approximate an ideal low-pass frequency response are of the form

$$T(P(s)) = \frac{\hat{K}}{\sum_{k=0}^{n} a_k P^k} \tag{A.2}$$

where $P = \cosh \sqrt{s}$.

They may also be written as

$$T(P(s)) = \frac{K}{\prod_{k=0}^{n} (P - \alpha_k)} \tag{A.3}$$

where $K = \hat{K}/a_n$ and the α_k are the roots of the denominator polynomial. It follows then that

$$|T(P(j\omega))| = \frac{|K|}{\prod_{k=0}^{n} (|P - \alpha_k|)} \tag{A.4}$$

where now $P = \cosh \sqrt{j\omega}$.

Now note that

$$|P - \alpha_k| \leq |P| + |\alpha_k| \ . \tag{A.5}$$

Thus,

$$|P - \alpha_k| < \left| \frac{e^{\sqrt{j\omega}} + e^{-\sqrt{j\omega}}}{2} \right| + \left| \alpha_k \right|$$

$$\leq \left| \frac{e^{\sqrt{j\omega}}}{2} \right| + \left| \frac{e^{-\sqrt{j\omega}}}{2} \right| + |\alpha_k|$$

$$\leq \left| \frac{e^{\sqrt{\frac{\omega}{2}}} e^{j\sqrt{\frac{\omega}{2}}}}{2} \right| + \left| \frac{e^{-\sqrt{\frac{\omega}{2}}} e^{-j\sqrt{\frac{\omega}{2}}}}{2} \right| + |\alpha_k|$$

$$|P - \alpha_k| \leq \frac{e^{\sqrt{\frac{\omega}{2}}}}{2} + \frac{e^{-\sqrt{\frac{\omega}{2}}}}{2} + |\alpha_k|. \qquad \text{(A.6)}$$

Now from stability considerations

$$1 \leq |\alpha_k| \leq 11.59 \qquad \text{(A.7)}$$

so

$$|P - \alpha_k| \leq e^{\sqrt{\frac{\omega}{2}}} + \frac{1}{2} + 11.59$$

$$\leq \frac{e^{\sqrt{\frac{\omega}{2}}}}{2} + 12.09. \qquad \text{(A.8)}$$

Now since

$$e^{\sqrt{\frac{\omega}{2}}} \geq 1 > \frac{12.09}{12.5} \tag{A.9}$$

$$12.5\, e^{\sqrt{\frac{\omega}{2}}} > 12.09$$

$$13\, e^{\sqrt{\frac{\omega}{2}}} > 12.09 + \frac{e^{\sqrt{\frac{\omega}{2}}}}{2} . \tag{A.10}$$

This implies that

$$|P - \alpha_k| < 13\, e^{\sqrt{\frac{\omega}{2}}} \tag{A.11}$$

and that

$$\prod_{k=0}^{n} (|P - \alpha_k|) < (13\, e^{\sqrt{\frac{\omega}{2}}})^n \tag{A.12}$$

This in turn implies that

$$|T(j\omega)| > \frac{|K|}{13^n}\, e^{-n\sqrt{\frac{\omega}{2}}} \tag{A.13}$$

and

$$|T(j\omega)|^2 > \frac{K^2}{13^{2n}}\, e^{-2n\sqrt{\frac{\omega}{2}}} . \tag{A.14}$$

To get a lower bound on the error from ω_o to $100\omega_o$ integrate the righthand side of (A.14).

$$\int_{\omega_o}^{100\omega_o} |T(j\omega)|^2 d\omega > \frac{K^2}{13^{2n}} \int_{\omega_o}^{100\omega_o} e^{-2n\sqrt{\frac{\omega}{2}}} d\omega$$

$$> \frac{K^2}{13^{2n} n^2} \left[e^{-2n\sqrt{\frac{\omega_o}{2}}} \left(2n\sqrt{\frac{\omega_o}{2}} + 1\right) - e^{-20n\sqrt{\frac{\omega_o}{2}}} \left(20n\sqrt{\frac{\omega_o}{2}} + 1\right)\right].$$

(A.15)

A lower bound on the second integral of equation (A.1) has now been obtained.

To find an upper bound on the last integral of equation (A.1) recall that

$$|T(j\omega)| = \frac{|K|}{\prod_{k=0}^{n} (|P - \alpha_k|)} . \qquad (A.4)$$

Now note that

$$|P - \alpha_k| \geq \left| |P| - |\alpha_k| \right| \qquad (A.16)$$

$$\geq \left| \left| \frac{e^{\sqrt{j\omega}} + e^{-\sqrt{j\omega}}}{2} \right| - |\alpha_k| \right|$$

Since the third integral in equation (A.1) concerns values of $\omega \geq 100\omega_o$ and since only values of $\omega_o \geq 1$ are of practical interest, it follows that

$$\frac{e^{\sqrt{\frac{\omega}{2}}}}{2} - 12.09 > 0 \tag{A.17}$$

for $\omega \geq 100\omega_o$.

Therefore,

$$|P - \alpha_k| > \left|\left| \frac{e^{\sqrt{j\omega}}}{2} \right| - \left|\frac{e^{-\sqrt{j\omega}}}{2}\right|\right| - |\alpha_k|\Big| \tag{A.18}$$

$$\geq \left|\frac{e^{\sqrt{\frac{\omega}{2}}}}{2} - \frac{e^{-\sqrt{\frac{\omega}{2}}}}{2} - |\alpha_k|\right|$$

$$|P - \alpha_k| \geq \left|\frac{e^{\sqrt{\frac{\omega}{2}}}}{2} - \frac{1}{2} - |\alpha_k|\right| . \tag{A.19}$$

Again, from stability considerations

$$1 \leq |\alpha_k| \leq 11.59$$

so

$$|P - \alpha_k| \geq \left|\frac{e^{\sqrt{\frac{\omega}{2}}}}{2} - 12.09\right| \tag{A.20}$$

Now note that for $\omega > 100\omega_o$

$$\frac{e^{\sqrt{\frac{\omega}{2}}}}{2} - 12.09 \geq e^{\sqrt{\frac{\omega}{8}} - \sqrt{\frac{100\omega_o}{8}}} \left[\frac{e^{2\sqrt{\frac{100\omega_o}{8}}}}{2} - 12.09\right] \qquad (A.21)$$

$$\frac{e^{\sqrt{\frac{\omega}{2}}}}{2} - 12.09 \geq e^{\sqrt{\frac{\omega}{8}}} \left[\frac{e^{\sqrt{\frac{100\omega_o}{8}}}}{2} - 12.09\, e^{-\sqrt{\frac{100\,\omega_o}{8}}}\right]. \qquad (A.22)$$

The expression inside the bracket on the right of (A.22) is a constant for any particular value of ω_o, therefore

$$\frac{e^{\sqrt{\frac{\omega}{2}}}}{2} - 12.09 \geq c e^{\sqrt{\frac{\omega}{8}}} \qquad (A.23)$$

where

$$c = \frac{e^{\sqrt{\frac{100\omega_o}{8}}}}{2} - 12.09\, e^{-\sqrt{\frac{100\omega_o}{8}}} . \qquad (A.24)$$

This implies that

$$|P - \alpha_k| \geq c e^{\sqrt{\frac{\omega}{8}}} \qquad (A.25)$$

and

$$\prod_{k=0}^{n} (|P - \alpha_k|) \geq (ce^{\sqrt{\frac{\omega}{8}}})^n \tag{A.27}$$

and

$$|T(j\omega)|^2 \leq \frac{K^2}{c^{2n}} e^{-2n\sqrt{\frac{\omega}{8}}} . \tag{A.28}$$

To get an upper bound on the error from $100\omega_o$ to infinity integrate the righthand side of (A.28).

$$\int_{100\omega_o}^{\infty} |T(j\omega)|^2 \, d\omega \leq \frac{K^2}{c^{2n}} \int_{100\omega_o}^{\infty} e^{-2n\sqrt{\frac{\omega}{8}}} \, d\omega$$

$$\leq \frac{4K^2}{c^{2n}n^2} [e^{-10n\sqrt{\frac{\omega_o}{2}}} (10n\sqrt{\frac{\omega_o}{2}} + 1)]. \tag{A.29}$$

Now divide the righthand side of (A.29) by the righthand side of (A.15) and define the quotient to be R.

$$R = \frac{\frac{4}{c^{2n}} [e^{-10n\sqrt{\frac{\omega_o}{2}}} (10n\sqrt{\frac{\omega_o}{2}} + 1)]}{\frac{1}{13^{2n}} [e^{-2n\sqrt{\frac{\omega_o}{2}}}(2n\sqrt{\frac{\omega_o}{2}} + 1) - e^{-20n\sqrt{\frac{\omega_o}{2}}} + 1)]} . \tag{A.30}$$

Now proceed to show that R<1. First, consider the term

$$e^{-2n\sqrt{\frac{\omega_o}{2}}}\left(2n\sqrt{\frac{\omega_o}{2}}+1\right)-e^{-20n\sqrt{\frac{\omega_o}{2}}}\left(20n\sqrt{\frac{\omega_o}{2}}+1\right). \quad (A.31)$$

This term can be rewritten as

$$e^{-2n\sqrt{\frac{\omega_o}{2}}}\left[\left(2n\sqrt{\frac{\omega_o}{2}}+1\right)-e^{-18n\sqrt{\frac{\omega_o}{2}}}\left(20n\sqrt{\frac{\omega_o}{2}}+1\right)\right]. \quad (A.32)$$

Now find the minimum value of the term inside the brackets of (A.32).

Let $x = n\sqrt{\frac{\omega_o}{2}}$ and define

$$g(x) = 2x + 1 - e^{-18x}(20x + 1) \quad (A.34)$$

$$g'(x) = 2-e^{-18x}[20 + (20x+1)](-18) \quad (A.35)$$

$$0 = 2 - e^{-18x}(2-360x). \quad (A.36)$$

Solving this equation reveals that x = 0 is the only solution. Now check to see if this is a minimum.

$$g''(x) = -e^{-18x}[-360 + (2-360x)(-18)]. \quad (A.37)$$

$$g''(0) = 396 > 0$$

This implies that the function g(x) has a minimum at x=0. But x=0 implies that either n=0 or ω_o=0, neither of which are permissible due to practical considerations. In fact,

$$n \geq 1$$
$$\omega_o \geq 1 \ . \qquad \text{(A.38)}$$

Thus, the minimum value of g(x) must be found subject to the constraints of (A.38). Now define

$$h(x) = 2x + 1 \qquad \text{(A.39)}$$

$$k(x) = e^{-18x} \ (20x + 1). \qquad \text{(A.40)}$$

Graphs of h(x) and k(x) are shown in Figure 19.

Now note that

$$h'(x) = 2 \qquad \text{(A.41)}$$

and that

$$k'(x) = e^{-18x}(2-360x) \qquad \text{(A.42)}$$

$$k''(x) = (5480x - 396) \ e^{-18x} \ . \qquad \text{(A.43)}$$

From (A.42) and (A.43), it is found that k(x) has a maximum at x = 1/180 and that the slope of k(x) is negative

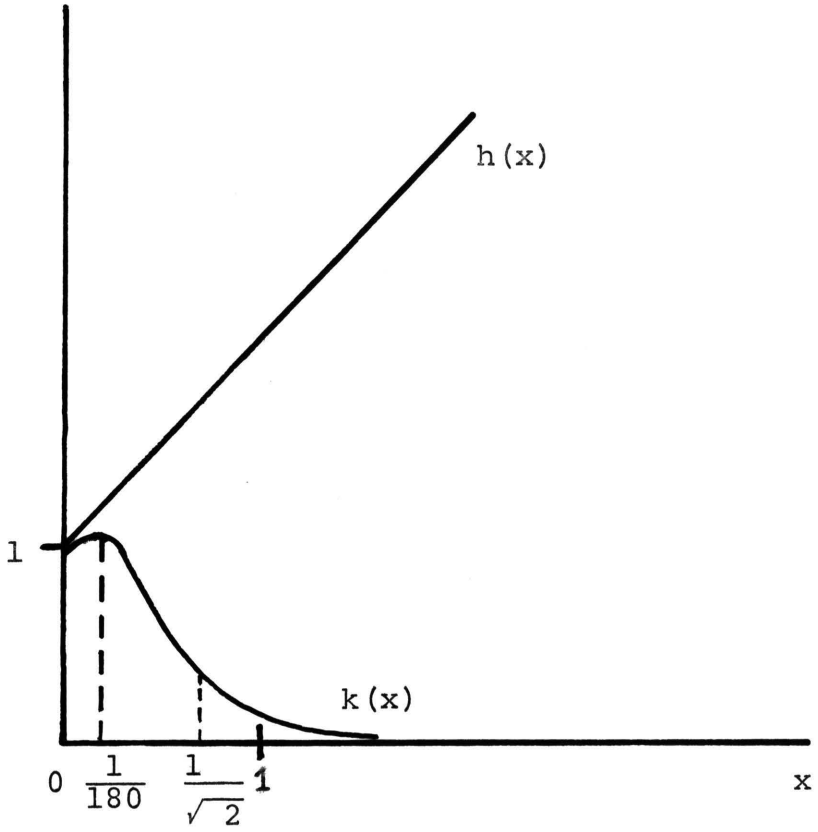

Figure 19. Graphs of h(x) and k(x)

for any x greater than 1/180. From (A.41) it is seen that the slope of h(x) is equal to 2, and from (A.38) it is found that the smallest feasible value of x is $\frac{1}{\sqrt{2}}$. Thus, it is concluded that for x greater than 1/180 the slopes of h(x) and k(x) are always opposite in sign; therefore, the smallest feasible value that h(x) - k(x) can achieve is at the smallest feasible x, that is, at $x = \frac{1}{\sqrt{2}}$.
Now returning to (A.31) it can be stated that

$$e^{-2n\sqrt{\frac{\omega_o}{2}}}\left(2n\sqrt{\frac{\omega_o}{2}} + 1\right) - e^{-20n\sqrt{\frac{\omega_o}{2}}}\left(20n\sqrt{\frac{\omega_o}{2}} + 1\right) =$$

$$e^{-2n\sqrt{\frac{\omega_o}{2}}}\left[\left(2n\sqrt{\frac{\omega_o}{2}} + 1\right) - e^{-18n\sqrt{\frac{\omega_o}{2}}}\left(20n\sqrt{\frac{\omega_o}{2}} + 1\right)\right] >$$

$$e^{-2n\sqrt{\frac{\omega_o}{2}}}\left[\left(2\sqrt{\frac{1}{2}} + 1\right) - e^{-9\sqrt{2}}\left(10\sqrt{2} + 1\right)\right] >$$

$$e^{-2n\sqrt{\frac{\omega_o}{2}}}\,[2.4]. \qquad \text{(A.44)}$$

Therefore it follows from (A.30) that

$$R < \frac{\frac{4}{c^{2n}}\left[e^{-10\sqrt{\frac{\omega_o}{2}}}\left(10n\sqrt{\frac{\omega_o}{2}}+1\right)\right]}{\frac{1}{13^{2n}}\left[2.4e^{-2n\sqrt{\frac{\omega_o}{2}}}\right]} \tag{A.45}$$

$$R < \frac{\frac{4}{c^{2n}}\left(10n\sqrt{\frac{\omega_o}{2}}+1\right)e^{-8n\sqrt{\frac{\omega_o}{2}}}}{\frac{1}{13^{2n}}(2.4)}. \tag{A.46}$$

Now consider the term

$$\left(10n\sqrt{\frac{\omega_o}{2}}+1\right)e^{-8n\sqrt{\frac{\omega_o}{2}}}. \tag{A.47}$$

Let $x = n\sqrt{\frac{\omega_o}{2}}$ and define

$$m(x) = 10xe^{-8x}. \tag{A.48}$$

It is found then that

$$m'(x) = e^{-8x}(10-80x) \tag{A.49}$$

and that the maximum value of m(x) occurs at x=1/8; but 1/8 is less than the minimum feasible value of x which is $\frac{1}{\sqrt{2}}$. Since the slope of m(x) is negative for x greater than 1/8, the maximum feasible value of m(x) is

$$m\left(\frac{1}{\sqrt{2}}\right) < .03. \tag{A.50}$$

Therefrom (A.46)

$$R < \frac{\frac{4}{c^{2n}}}{\frac{1}{13^{2n}}}.0125 \tag{A.51}$$

$$R < .05 \left(\frac{13}{c}\right)^{2n} . \tag{A.52}$$

Now recall from (A.24) that

$$c = \frac{e}{2}^{\sqrt{\frac{100\omega_o}{8}}} - 12.09\ e^{-\sqrt{\frac{100\omega_o}{8}}} \tag{A.24}$$

Now let $x = \sqrt{\frac{100\omega_o}{8}}$ and define

$$r(x) = \frac{e^x}{2} - 12.09\ e^{-x} \tag{A.53}$$

$$r'(x) = \frac{e^x}{2} + 12.09\ e^{-x}. \tag{A.54}$$

From (A.53) and (A.54) it can be concluded that r(x) has no minimum on the interior of the interval $[0,\infty]$. But since r(x) increases monotonically the minimum value of r(x)

is r(x) evaluated at the minimum feasible value of x, which is 3.56. Therefore

$$r(3.56) > 17 . \tag{A.55}$$

Thus from (A.52)

$$R < .05(\frac{13}{17})^{2n}. \tag{A.56}$$

Thus since $n \geq 1$

$$R < .03. \tag{A.57}$$

Thus it is concluded that since $R < .03$, the area contributed by the third integral of equation (A.1) is insignificant compared with the values of the other two integrals. This allows the third integral of (A.1) to be ignored and then (A.1) can be written as

$$\text{I.S.E.} \simeq \frac{\omega_o^2+100}{\omega_o^2} \left[\int_o^{\omega_o} [1 - |T(j\omega)|]^2 d\omega + \int_{\omega_o}^{100\omega_o} |T(j\omega)|^2 d\omega\right] \tag{A.58}$$

and this corresponds to equation (3.10). By a similar line of reasoning the same result can be shown for the w-plane.